Palaeogeography, Palaeoclimatology, Palaeoecology 659 (2025) 112627

Contents lists available at ScienceDirect

Palaeogeography, Palaeoclimatology, Palaeoecology

journal homepage: www.elsevier.com/locate/palaeo

Making sense of variation in sclerochronological stable isotope profiles of mollusks and fish otoliths from the early Eocene southern North Sea Basin

Johan Vellekoop [a,b,*], Daan Vanhove [a,b], Inge Jelu [a,b], Philippe Claeys [c], Linda C. Ivany [d], Niels J. de Winter [c,e], Robert P. Speijer [a], Etienne Steurbaut [b,a]

[a] Department of Earth and Environmental Sciences, KU Leuven, 3001 Heverlee, Belgium
[b] OD Earth and History of Life, Institute of Natural Sciences, 1000 Brussels, Belgium
[c] Archaeology, Environmental changes and Geo-Chemistry, Vrije Universiteit Brussel, 1050 Brussels, Belgium
[d] Department of Earth and Environmental Sciences, Heroy Geology Laboratory, Syracuse University, Syracuse, NY 13244-1070, USA
[e] Faculty of Science, Vrije Universiteit Amsterdam, 1081 HV Amsterdam, Netherlands

ARTICLE INFO

Editor Name: Prof. M Elliot

Keywords:
Sclerochronology
Fossil assemblage
Eocene
Taphonomy

ABSTRACT

Stable isotope sclerochemistry of biogenic carbonate is frequently used for the reconstruction of paleotemperature and seasonality. Yet, few studies have compared intra-and inter-taxon isotope variability and variation within a single depositional environment. We measured seasonal changes in $\delta^{18}O$ and $\delta^{13}C$ compositions in multiple specimens of two carditid bivalve species, a turritelline gastropod species, and two species of otoliths from demersal fish, from two early Eocene (latest Ypresian, 49.2 Ma) coquinas in the inner neritic Aalter Formation, located in the Belgian part of the southern North Sea Basin (paleolatitude ~41°N). Results demonstrate considerable variation among taxa in the mean, amplitude, and skewness of $\delta^{18}O$ and $\delta^{13}C$ values from sequentially sampled growth series. We attribute this variation to factors including differences in seasonal growth over ontogeny, mixing of depositional settings by sediment transport, differences between sedentary and mobile organisms, and differences in longevity of the taxa in question. Growth cessation during winters in turritellines and fishes in particular lead to an incomplete representation of the seasonal cycle in their growth increments, in comparison to carditid bivalves. Ophidiid fish otolith isotope records appear to reflect environmental conditions over a wider range of habitats and environments, and we infer this is due to a combination of sedimentary transport, as these are small structures, and postmortem transport by free-swimming predatory fish. Our study highlights the potential variability encompassed by taxa in the shallow marine realm even when they are found in the same deposits. While this has significant implications for seasonality reconstructions based on conventional isotope profiles, we show that careful study of the ecology and ontogeny of multiple taxa and specimens within a death assemblage can reveal sources of variation and yield a close approximation of conditions in the setting of interest.

1. Introduction

Reconstructions of past warm climates deliver essential information on the response of Earth's climate system to warming (Burke et al., 2018; Tierney et al., 2020). Datasets of past climate help us to assess the ability of climate models to simulate warm climate scenarios, aiding in the improvement of future climate projections (Calvin et al., 2023). Short-term archives of past climate, such as the incrementally mineralized parts of mollusks (shells) and fish (otoliths) enable us to reconstruct climate variability on the seasonal timescale (Ivany, 2012). Oxygen isotope sclerochemistry has become a widely applied tool for the reconstruction of intra-annual variation in ambient temperature and water composition (e.g. Williams et al., 1982; De Winter et al., 2018, 2020; Clark et al., 2022; Ivany and Judd, 2022; Kniest et al., 2024). Carbon isotope composition of accretionary archives is explored to a lesser degree but contributes to our understanding of species metabolism and diet, and variations in primary productivity and dissolved inorganic carbon (DIC) compounds in water (e.g. McConnaughey and Gillikin, 2008; Van Horebeek et al., 2021; Clark et al., 2022). For seasonal-scale climate reconstructions of the high-CO_2 Paleogene greenhouse world,

* **Corresponding author at:** Department of Earth and Environmental Sciences, KU Leuven, 3001 Heverlee, Belgium.
E-mail address: johan.vellekoop@kuleuven.be (J. Vellekoop).

https://doi.org/10.1016/j.palaeo.2024.112627
Received 28 June 2024; Received in revised form 16 October 2024; Accepted 24 November 2024
Available online 30 November 2024

considered as an analogue for a 'worst case scenario' for anthropogenic global warming (Tierney et al., 2020), commonly used fossil groups include turritellid gastropods (e.g. Andreasson and Schmitz, 1996, 1998, 2000; Kobashi et al., 2001, 2004; Ivany et al., 2018) and carditid bivalves (e.g. Purton and Brasier, 1999; Kobashi et al., 2001, 2004; Ivany et al., 2004; Keating-Bitonti et al., 2011; Vanhove et al., 2012; Sessa et al., 2012; Kniest et al., 2024). In addition, fossil otoliths are also regularly utilized, in particular those from non-migratory groundfish such as ophidiids (Vanhove et al., 2011, 2012) and congrids (Kobashi et al., 2004; Ivany et al., 2000, 2003; De Man et al., 2004; Vanhove et al., 2011, 2012). Because these groups are thought to be benthic and non-migratory throughout their lifespan, they are expected to record the seasonality within a single environment.

Taxon-specific differences in mode of life, preferred habitat and season of growth, however, mean that different types of skeletal archives in a single death assemblage may not uniformly record similar ambient conditions. Moreover, fossil assemblages are also influenced by a variety of taphonomic and sedimentological processes, potentially introducing additional isotopic variability. Few studies have directly compared intra-and inter-taxon isotope variability and variation within a single fossil assemblage to test whether different fossil groups record the same isotopic seasonality. Therefore, to test the similarity of sclerochronological stable isotope profiles of different Paleogene taxa, this study focuses on seasonal variation within and variability among incremental $\delta^{18}O$ and $\delta^{13}C$ profiles of a turritelline gastropod species (*Haustator solanderi*), two species of carditid bivalves (*Venericor planicosta lerichei* and *Cyclocardia (Arcturellina) sulcata aizyensis*) and otoliths from two species of demersal non-migratory fish, the congrid *Paraconger sauvagei* and the ophidiid '*Neobythites*' *subregularis* (Fig. 1). All fossils are derived from two successive upper Ypresian shallow marine coquina beds in the inner neritic Aalter Formation (Zenne Group), outcropping in the Belgian part of the southern North Sea Basin (sNSB). The lower coquina bed contains abundant large *Venericor* bivalve shells, while the upper one contains abundant *Haustator* gastropods. Each coquina was likely deposited within hundreds to possibly thousands of years, while the succession *en toto* probably represents a time span of several tens of thousands of years. Hence, all fossils are derived from a narrow, stratigraphically well-constrained interval, corresponding in time to the latest Ypresian, at ~49.2 Ma (Steurbaut and Nolf, 2021), just after the Early Eocene Climatic Optimum (EECO; Zachos et al., 2008; Evans et al., 2018; Speijer et al., 2020). Hence, it can be assumed that similar climatological conditions and environmental settings prevailed during deposition of both coquina beds.

We assess differences in amplitude and mean of intra-annual isotope variability among specimens and species from the Aalter Formation coquina beds, and discuss potential environmental, biological, ecological and taphonomical causes for these differences. Our findings lead to insights about the significance of isotopic variability among different types of skeletal archives in a death assemblage from a shallow marine setting, constraining their value as proxy archives of seasonality.

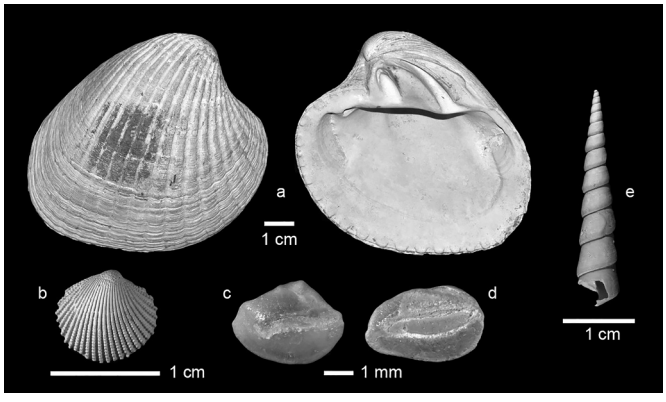

Fig. 1. Representative specimens of taxa from the Aalter Fm. used in this study: (a) *Venericor planicosta lerichei*, specimen B13D; (b) *Cyclocardia* (*Arcturellina*) *sulcata aizyensis*, specimen B9B; (c) *Paraconger sauvagei*, specimen O205B; (d) '*Neobythites*' *subregularis*, specimen O207B; (e) *Haustator solanderi*, specimen B11H.

2. Geological context

The Aalter Sand Formation consists of a grey green, glauconiferous, clayey fine sand, locally with fine sandy clay layers and a few thin poorly cemented sandstone layers, which passes into very fossiliferous, fine grey sand at the top (Steurbaut and Nolf, 1989). It crops out locally in northwestern Belgium in the Gent-Aalter-Oedelem area and in a series of small hills 60 km to the southwest along the French-Belgian border (Scherpenberg, Cassel, Mont-des-Récollets), and occurs in the subsurface in the southwestern part of the Netherlands and offshore on the Belgian continental shelf (Le Bot et al., 2003; Steurbaut and Nolf, 2021). In the mid-1800's, first descriptions of fossils in the Aalter Sand Formation appeared in field trip reports, emphasizing the abundance of turritellines and large *'Cardita (Venericardia) planicosta'* shells near the Aalter train station in Belgium (e.g. Nyst and Mourlon, 1871). Today, parts of the Aalter Sand Fm. are occasionally exposed during construction works in the Aalter region.

This study is limited to two coquinas in the Oedelem Member of the Aalter Sand Formation (Steurbaut and Nolf, 1989; King, 2016), cropping out in the Aalter stratotype area. These coquinas correspond to the interval with '*Megacardita planicosta lerichei*' [now *Venericor planicosta lerichei* (Gilbert and van de Poel, 1970)] and the interval with '*Turritella solanderi*' [now *Haustator solanderi* (Mayer-Eymar, 1877)], layers 2–3 and layers 4–7 in Steurbaut and Nolf (1989) (Fig. 2), respectively. Henceforth, the two coquinas are referred to as the 'venericard' and 'turritelline' layers. They are both composed of olive-green fine-to-medium grained and locally coarse sands with glauconite and abundant mollusks. Most shells of *V. planicosta lerichei* are disarticulated, but some are still articulated, suggesting rapid post-mortem burial (Steurbaut and Nolf, 1989). In the turritelline layer, about 90 % of the macrofossils

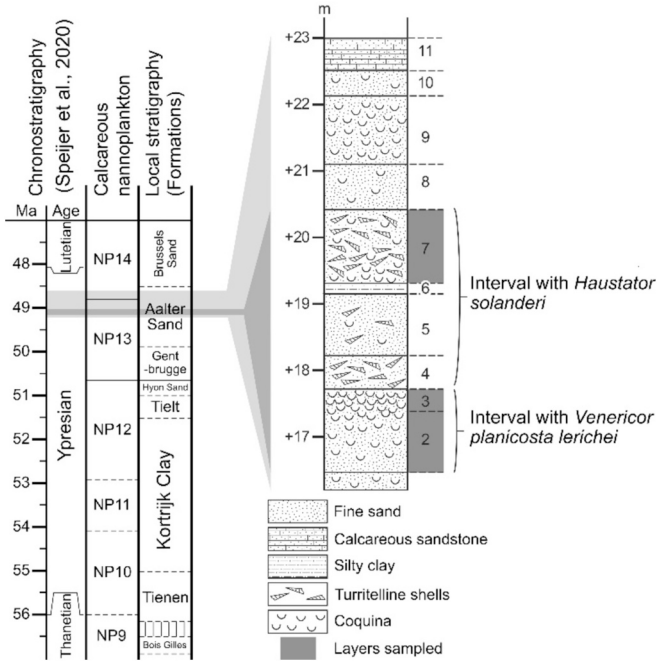

Fig. 2. Part of the stratotype of the Aalter Fm. at Aalter, Belgium (modified after Steurbaut and Nolf, 1989). The layers containing the specimens used in this study correspond to layers 2–3 and 7 of the stratotype, correlated to the chronostratigraphic timescale.

belong to *H. solanderi*. Other constituents in the Aalter Sand Fm. fauna include benthic foraminifera, bryozoans, irregular echinoids, solitary corals, serpulid worm tubes, other gastropods and bivalves, cephalopod fragments, teleost fish otoliths and bone fragments, and chondrichthyan teeth (Nyst and Mourlon, 1871; Kaasschieter, 1961; Nolf, 1972a; Steurbaut and Nolf, 1989). The coquina beds are separated by an omission surface, implying that the venericard layer belongs to the top of Unit A2 and the turritelline layer to the lower middle part of Unit A3, as defined in Steurbaut and Nolf (2021). Calcareous nannofossil assemblages are indicative for the upper part of Zone NP13 (Steurbaut and Nolf, 1989, 2021). The first occurrences of *Discoaster* cf. *sublodoensis* (a few corroded *D. sublodoensis*-like specimens) and *Discoaster praebifax* are situated close to the base of the turritelline layer (Steurbaut and Nolf, 1989; King, 2016), while the last occurrences of *Nannoturba jolotteana* and *N. spinosa* occur above the venericard layer (Steurbaut and Nolf, 2021), placing the studied interval in upper Subzone NP13b to lower Subzone NP13c of Steurbaut and Nolf (2021). The first occurrence of *Discoaster sublodoensis* s.s., which is part of the major calcareous nannofossil turnover around the Ypresian-Lutetian boundary (Steurbaut and Nolf, 2021), occurs several meters above the studied interval, in the upper part of the Aalter Sand stratotype. The age of the coquinas is therefore latest Ypresian, around 49.2 Ma, with respect to the Paleogene time scale (Speijer et al., 2020).

3. Paleoenvironment and paleogeography

3.1. Paleoenvironment

The general environmental model for the late Ypresian – early Lutetian in the Belgian part of the sNSB is an advancing and retreating deltaic system (Jacobs et al., 1991; Jacobs and Sevens, 1993; Gibbard and Lewin, 2016). The combination of sediment supply from this delta and sea-level variations led to an array of highly diverse facies representing inner neritic, sublittoral, intertidal, barrier, lagoonal and estuarine deposits (Jacobs et al., 1991). The Aalter Sand Formation consequently exhibits a large facies diversity, both vertically and laterally (Jacobs and Sevens, 1993), reflecting these varying sedimentary environments. Nonetheless, the presence of glauconite, characteristic sedimentology and diagnostic fossil content, including calcareous nannoplankton assemblages indicative of shallow water conditions (Steurbaut and Nolf, 1989; Jacobs and De Batist, 1996), unambiguously establish deposition in a very shallow marine, littoral or sublittoral environment. The overall otolith assemblage occurring in the Aalter Sand Fm. (Nolf, 1972a) is in agreement with this. While modern *Paraconger* has been recorded from 10 to 75 m (Kanazawa, 1961) and ophidiids occur from shelf to abyssal depths (FishBase, 2023), recent relatives of the genera *Orthopristis*, *Platycephalus* and *Apogon*, all present in the Aalter assemblage (Nolf, 1972a), occur in very proximal habitats (FishBase, 2023). The nannofossils (Steurbaut and Nolf, 1989), otolith assemblage (Nolf, 1972a), mollusk assemblages (Nyst and Mourlon, 1871; Glibert, 1985) and presence of solitary corals and cephalopod fragments (Steurbaut and Nolf, 1989), together with storm-induced winnowing and occasionally subtle channeling in the venericard coquina, all suggest a shallow, inner neritic depositional setting, above fair-weather base (Jacobs and Geets, 1977), probably less than 30 m deep, with generally fully marine, normal salinity conditions.

Jacobs and Sevens (1993) interpreted the sequence of the Oedelem Member of the Aalter Sand Fm. in boreholes offshore the current Belgian coast as a submerged coastal barrier, followed by storm deposits in a lagoonal environment, as evidenced by partially incising fine sands with centimeter thick clay layers and flaser lamination. The accumulations of venericard and turritelline shells were interpreted to reflect either storm or chenier (see Cangzi and Walker, 1989) deposits. Nevertheless, in the stratotype area, the Aalter Sand Formation contains less clay, and flaser bedding was not observed (Jacobs and Geets, 1977; Steurbaut and Nolf, 1989), with granulometry indicating non-uniform low-turbulence suspension (Jacobs and Geets, 1977). These results are more consistent with a subtidal channel system, potentially with lagoons or mudflats relatively nearby. The coquina beds likely represent concentrations of shells on the bottom of these channels, resulting from winnowing and/or storms (Steurbaut and Nolf, 1989; Jacobs, 2015).

3.2. Paleoceanography

The paleolatitude of Aalter is ~41°N (Van Hinsbergen et al., 2015). During the Eocene, the sNSB area shared similarities with today's configuration as a partly enclosed, shallow siliciclastic shelf environment. However, it differed in terms of the number and position of connections to the open ocean (Fig. 3). In the late Ypresian to early Lutetian, the sNSB probably opened northward to the Atlantic Ocean and Arctic waters via the Viking Graben and Norwegian Seaway (Knox et al., 2010; Gibbard and Lewin, 2016). In addition, microfossil evidence and the presence of several fish taxa primarily associated with the Indo-West-Pacific region, including the genus *Platycephalus*, provide support for an early to mid-Ypresian connection between the sNSB and the Tethys region to the southeast (Nolf, 1972b; Steurbaut and Nolf, 1990; Steurbaut, 2011; Knox et al., 2010; King, 2016). Evaluating whether this eastward connection maintained during the late Ypresian proves challenging, as the discrepancies in calcareous nannofossil content between the North Sea Basin and the Peritethys during that time could either indicate a severed connection or the emergence of distinct paleoenvironmental settings (Steurbaut, 2011; King, 2016).

From the late Ypresian onwards, the southward connection with the Atlantic Ocean was impacted by tectonically controlled uplift related to the renewal of Africa-Europe convergence. This uplift, for example indicated by the erosive bases of the nearby Egem Member and Brussels Fm., caused restricted connection between the Belgian and Paris Basins (Vandenberghe et al., 2004). King (2006) however, in support of an 'open' configuration for the sNSB, lists several lines of evidence for continued interchange with the Atlantic, most importantly the presence of warm-water nummulites in the sNSB and the fact that no physical barrier is required to explain differences in facies between the London and Hampshire Basins. Two possible options for a southward connection with the Atlantic are through the English Channel or, if this channel would have been blocked by uplift of the Start-Cotentin Swell, via the Loire Seaway, between the Amorican massif and France in Fig. 3 (Gély, 2008; Knox et al., 2010; Huyghe et al., 2012). Regardless, during the early Eocene sNSB region likely became increasingly enclosed, possibly influencing the local sea water isotopic composition ($\delta^{18}O_{sw}$, Kniest et al., 2024).

4. Methods

4.1. Specimen collection

Specimens were retrieved from field sampling and from the collections of the Belgian Institute of Natural Sciences (INS; see Table 1 and Fig. 1). In 2010, about 3 m of the Aalter Sand Fm. below layer 11 (Steurbaut and Nolf, 1989) was exposed in a construction pit located in the village center (Hagepreekstraat, Aalter, Appendix A). The lower part of the exposure contained abundant *H. solanderi* and is therefore thought to correspond to layer 7 in the Aalter Sand Fm. stratotype description of Steurbaut and Nolf (1989). Most of the specimens studied here were selected from a 30 kg sediment sample residue of this turritelline coquina, including six *H. solanderi* specimens, one specimen each of the otoliths from *Paraconger sauvagei* (Priem, 1906) and '*Neobythites*' *subregularis* (Schubert, 1916), and nine small carditids belonging to *Cyclocardia (Arcturellina) sulcata aizyensis* (Deshayes, 1858). Taxonomy of otoliths is according to Lin et al. (2017). When otolith genera are written with quotation marks it concerns a morphologically delineated species that cannot be assigned to a specific genus, but only to a higher rank, in this case, the subfamily Neobythitinae. However, because of the demand

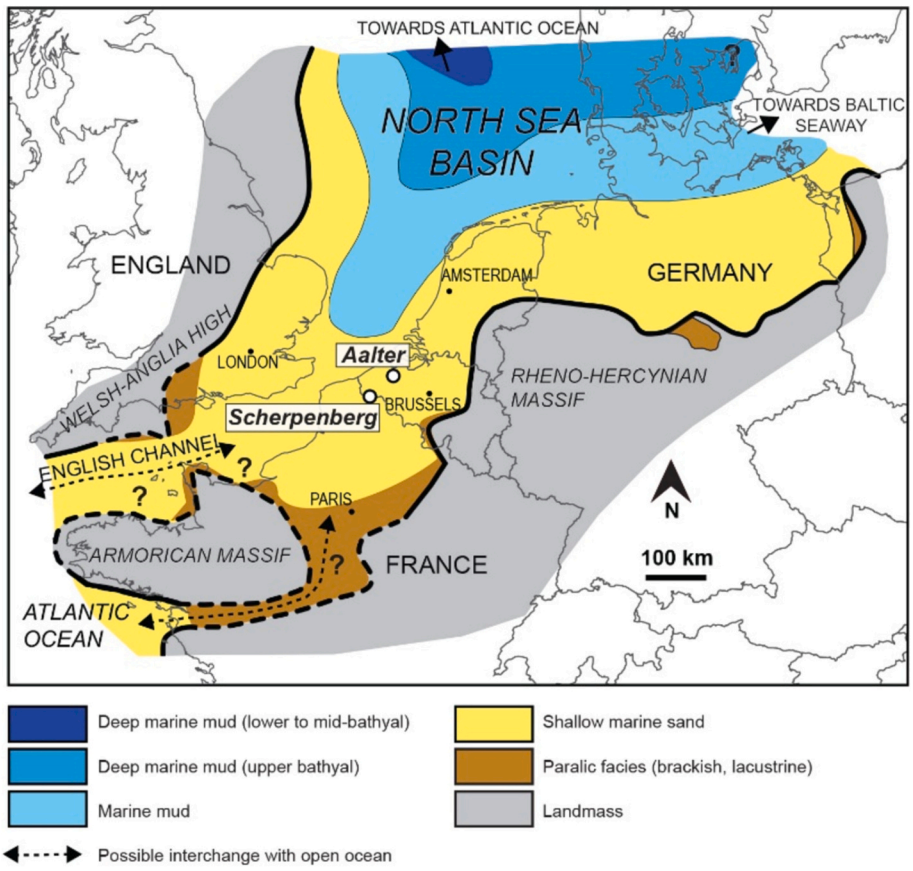

Fig. 3. Paleogeographic reconstruction of the southern North Sea Basin area during the latest Ypresian to early Lutetian, based on and modified from (Murray, 1992; King, 2006; Gély, 2008; Knox et al., 2010; Huyghe et al., 2012; Steurbaut et al., 2016). The basin had two connections with the Atlantic Ocean, one to the north and one to the southwest. There are two potential options for a southwestern gateway, one via the English Channel and the other south of the Armorican Massif ('Loire Seaway').

for adopting a strictly binomial nomenclature, '*Neobythites*' is now preferred above "genus *Neobythitinorum*", a term formerly used in Vanhove et al. (2011, 2012). Additional specimens of *P. sauvagei* and '*N.*' *subregularis*, one of each (O205B and 0208B), were selected from the INS fish otolith collection, collected around 1970 by dr. Dirk Nolf in the turritelline coquina, a few hundred meters west of our sample locality (Nolf, 1972b). From the venericard layer, three large *Venericor planicosta lerichei* (Gilbert and van de Poel, 1970) specimens were selected from the INS invertebrate collection. Previously published results from two ophidiid specimens (Vanhove et al., 2011) from the Aalter Sand Fm. at Scherpenberg (O2B; O2D; Fig. 3) are included in the dataset and the results section, to facilitate data comparison and to provide a more complete view of the lateral isotopic variability in the Aalter Sand Fm. The Scherpenberg locality is located 56 km SW of Aalter and precise correlation with the stratotype in the Aalter locality has not been attempted (Nolf, 1972a).

4.2. Assessing preservation

The sediments of the Aalter Sand Fm. are unlithified and have not been buried deeply since deposition, and and aragonitic fossils abound. Previous studies have demonstrated the excellent preservation of otoliths from the Ypresian deposits in Belgium, including from the Aalter Sand Fm. at Scherpenberg, using scanning electron microscopy (SEM), cold cathode luminescence microscopy and X-ray diffraction (XRD) analyses (e.g. Vanhove et al., 2011). In order to confirm the preservation state of the specimens studied here, we performed optical microscopy on all studied specimens. To confirm original aragonite mineralogy XRD analyses on powdered fragments from *H. solanderi* and *V. planicosta lerichei* specimens from Aalter and a '*N.*' *subregularis* specimen from Scherpenberg, by means of a Philips PW 1830 Generator (Cu-Kα, 30 mA, 45 Kv, 15–55° detection) were performed at the Department of Earth and Environmental Sciences (KU Leuven), using Topas Academic V4 software for comparison with standard patterns. In addition, the same specimens of *H. solanderi* and *V. planicosta lerichei* from Aalter were also investigated using Scanning Electron Microscopy (SEM; Jeol JSM-6400) to assess shell microtextures.

4.3. Microsampling and isotope analysis

Before microsampling, all specimens were ultrasonically rinsed in deionized water. Otoliths were embedded with an automated mounting press and polished manually on wetted sand-paper until slightly above the sagittal plane such that a maximum surface and depth is available for microsampling (see Vanhove et al., 2011).

Venericor planicosta lerichei bivalves were embedded in epoxy resin manually, cut with a wetted slow-speed saw (Syracuse University, NY) and finely polished to reveal growth features. Otoliths and *V. planicosta lerichei* bivalves were sampled with a Merchantek (currently ESI) micromilling device with 0.1 mm (Brasseler®) or 0.3 mm (Dremel®) drill bits (Vrije Universiteit Brussel, VUB). Incremental samples were drilled parallel to growth increments and represent continuous series. In otoliths, approximately ¾ of the surface of the sagittal plane was sampled, by taking concentric samples following the growth increments, from nucleus to edge, obtaining the entire ontogeny for each specimen. In *V. planicosta lerichei*, growth increments, presumably corresponding to years, suggest that specimen B13D lived for 13+ years, whereas specimen B14E lived for 9 years. For both specimen, three successive

Table 1
Collection and sample metadata for the specimens used in this study, retrieved from field sampling and museum collections.

ID*	Species	Family	Locality	Collection	Lithostratigraphy	Sample type
	Otoliths:					
O205B	*Paraconger sauvagei*	Congridae	Aalter, B., Rijksmiddelbare school, Stationstraat	INS** Otolith collection	Level with *H. solanderi*	Increments
O206A	*Paraconger sauvagei*	Congridae	Aalter, B., Hagepreekstraat	New sampling	Level with *H. solanderi*	Increments
O207B	*'Neobythitina' subregularis*	Ophidiidae	Aalter, B., Hagepreekstraat	New sampling	Level with *H. solanderi*	Increments
O208B	*'Neobythitina' subregularis*	Ophidiidae	Aalter, B., Rijksmiddelbare school, Stationstraat	INS Otolith collection	Level with *H. solanderi*	Increments
O2B***	*'Neobythitina' subregularis*	Ophidiidae	Scherpenberg, B.	INS Otolith collection		Increments
O2D***	*'Neobythitina' subregularis*	Ophidiidae	Scherpenberg, B.	INS Otolith collection		Increments
O2E	*'Neobythitina' subregularis*	Ophidiidae	Scherpenberg, B.	INS Otolith collection		XRD only
	Gastropods:					
O11A, C, E, F, G, H	*Haustator solanderi*	Turritellidae	Aalter, B, Hagepreekstraat	New sampling	Level with *H. solanderi*	Increments
	Bivalves:					
B13B	*Venericor planicosta*	Carditidae	"Aeltre, abri face à la maison communale"	RBINS Invert-13,660-0002	Level with *V. Planicosta*	Bulk lines
O13D	*Venericor planicosta*	Carditidae	"Aeltre, abri face à la maison communale"	RBINS Invert-13,660-0004	Level with *V. Planicosta*	Increments
O14E	*Venericor planicosta*	Carditidae	"Aeltre"	RBINS Invert-03280-0001	Level with *V. Planicosta*	Increments
B9A, B, C, D, E, F, H, I, J	*Cyclocardia (Arcturellina) sulcata aizyensis*	Carditidae	Aalter, B, Hagepreekstraat	New sampling	Level with *H. solanderi*	bulk

* For specimens O1A, O1B, O2A, O2B, O2C & O2D, see Vanhove et al., 2011.
** INS = Institute of Natural Sciences.
*** from Vanhove et al. (2011).

major increments were selected and sampled in the umbonal region. Sampling a limited number of years from multiple specimens captures interannual variation on the time scale of the shell bed better than sampling many years in a single individual, and accounts for taphonomic redistribution and averaging of the depositional time window (Goodwin et al., 2003). Three well-preserved years were serially sampled from the adult portions of the ontogeny of two individuals, years 9–11 in B13D and years 6–8 in B14E. While seasonal variation in growth rate could be more apparent later in ontogeny than in early years, the ShellChron approach discussed below accommodates and corrects for such variation. Bulk samples were taken in specimen B13B by drilling approximately linear paths perpendicular to all growth lines, in the middle part of the ventral region. As *Cyclocardia (A.) sulcata aizyensis* specimens are smaller than 1 cm in diameter, only bulk samples could be generated, by taking a subsample of powder resulting from crushing and homogenizing the entire shell.

Haustator solanderi specimens were sampled along the whorls with a Dremel® hand-held drill progressively at constant angles of mostly 180° or 90° along the outer shell from apex to aperture. Specimens B11F and B11H were sampled with a resolution of four samples per whorl, while only two samples per whorl were drilled in specimens B11A, B11C, B11E and B11G. Specimen B11A could not be fully sampled because the first series of whorls broke off during microdrilling; two other specimens had incomplete apexes (B11C, B11G), impeding a sampling of the first whorls.

The mass of the microsampled aragonite powders varied between 40 and 80 μg, and samples were analyzed in the stable isotope laboratory of the VUB with a ThermoFinnigan Kiel III coupled to a DeltaPlusXL mass spectrometer. Average precision based on NBS19 replicates is 0.02 ‰ for carbon and 0.05 ‰ for oxygen. Several replicate samples of the *C. (A.) sulcata aizyensis* specimens were run in the stable isotope lab of the University of Michigan, Ann Arbor, MI, with a Kiel IV coupled to a ThermoFinnigan MAT 253 mass spectrometer. Results are reported in ‰ VPDB, and values for δ18Ow in ‰ VSMOW. Raw results of all analyses are listed in Supplement S1.

For statistical comparison among results from different taxa, the unpaired *t*-test for equal means was used, unless the F-test indicated unequal variances, in which case the Welsh test was used. Significance level α was 0.05 in all cases.

The ShellChron 0.4.0 model (De Winter, 2022), based on the approach of Judd et al. (2018), was used in R (R version 4.3.1, Rstudio version 2023.06.0 build 421) to transfer $\delta^{18}O_c$ data to the time domain (Julian days), using a combination of growth rate and temperature sinusoid models on the isotope records while applying a sliding window approach. For this, the model assumes that growth and temperature follow quasi-sinusoidal patterns (Judd et al., 2018; De Winter, 2022). Since variability in $\delta^{18}O_w$ is comparatively limited in most fully marine environments (Rohling, 2013), the $\delta^{18}O_c$ record preserved in the accretionary shells of extra-tropical mollusks can offer a good approximation of seasonal temperature fluctuations so long as seasonal changes in growth rate are taken into account (Judd et al., 2018; Ivany and Judd, 2022; De Winter, 2022).

5. Results

5.1. Preservation

Optical microscopic examination reveals that, while otoliths from the Aalter Sand Formation do show slight signs of surface abrasion, the fossils from this formation are generally well-preserved. The *V. planicosta lerichei* shells show clear macroscopic growth increments. XRD of powdered fragments from *H. solanderi* and *V. planicosta lerichei* specimens from Aalter and a '*N.*' *subregularis* specimen from Scherpenberg, indicate that they are composed entirely of aragonite (Appendix

B). SEM images of the same *H. solanderi* and *V. planicosta lerichei* specimens from Aalter reveal ultrastructures similar to those of modern specimens (Appendix B). It is therefore unlikely that the aragonite shells and otoliths from the Aalter Sand Fm. are significantly affected by dissolution and/or chemical alteration.

5.2. $\delta^{18}O$ results

Distinct intra-annual variation is observed in all $\delta^{18}O$ profiles, with a total range over all specimens of 4.7 ‰, from −5.5 to −0.8 ‰ (Figs. 4–7). The results of the ShellChron 0.4.0 model reveal seasonal fluctuations of oxygen isotope values throughout the year within species, while also depicting the variation among their reconstructions (Fig. 8).

Stable oxygen isotope profiles of the large carditid bivalve *V. planicosta lerichei* reveal prominent, and relatively consistent, cyclical variation. The shape of the profile is sinusoidal for years sampled earlier in ontogeny and more saw-toothed for years later in ontogeny. Values in both specimens range from about −1.5 to −5.3 ‰, spanning the largest range in intra-annual values observed for all taxa. The average of the 5 % lowest values is −5.28 ‰, the 5 % highest values is −1.60 ‰. The species mean for *V. planicosta lerichei* is −3.6 ‰. Consistent with previous studies on *Venericor* specimens (e.g. Purton et al., 1999; Ivany et al., 2004; Kniest et al., 2024), the spacing between years 9–11 in B13D is narrower than between years 6–8 in B14E, likely highlighting an ontogenetic slowdown in growth. Nonetheless, a restriction in amplitudes of seasonal $\delta^{18}O$ variation (as for example seen in Ivany et al., 2004) is minimal, with average minimum and maximum δ18O values comparable. Results of whole shell analyses of the small carditid bivalve *C. (A.) sulcata aizyensis* vary between −2.4 and − 5 ‰ and show a species average of −3.3 ‰ (see Supplement S1). The average of the 5 % lowest values is −5.05 ‰, the 5 % higher values is −2.34 ‰. While this range of values falls within the range of *V. planicosta lerichei*, it is striking that the different *C. (A.) sulcata aizyensis* specimens have such large differences in average values. The oxygen isotope values of subsamples from the turritelline gastropod *H. solanderi* range between −2.5 and − 5.1 ‰, with a species average of −4.1 ‰. The average of the 5 % lowest values is −4.80 ‰, the 5 % higher values is −2.97 ‰. The average intra-annual range of this species is 1.7 ‰, smaller than the other studied taxa. Nevertheless, the amplitude of variation varies considerably between different *H. solanderi* shells, ranging from 2.2 ‰ in B11C to just 1.3 ‰ in B11G. The profiles of *H. solanderi* are more variable and less consistent in terms of shape and cyclicity compared to the bivalves from this location. Some specimens (B11F, B11C, B11E) show a cuspate pattern, with sharp peaks and broad troughs. In otoliths from Aalter, cyclicity is most pronounced in the two congrid specimens, with values ranging between −2.2 and − 4.5 ‰, and a species average of −3.5 ‰. The average of the 5 % lowest values is −4.51 ‰, the 5 % higher values is −2.19 ‰. The oxygen isotope profiles are again relatively cuspate. The two ophidiid specimens from Aalter are characterized by values in between −1.8 and − 3.4 ‰ and a species average of −2.5 ‰, a smaller range and more positive values in comparison with the congrid specimens. The lowest value is −3.43 ‰, the highest values is −1.82 ‰. Two ophidiid specimens from the Scherpenberg locality (Vanhove et al., 2011) have an intra-annual range between −0.8 and − 5.5 ‰, larger than the Aalter ophidiid and congrid specimens, and show a species average of −2.8 ‰, lower than the ophidiids from Aalter. The taxon means of the two species of carditid bivalves (*V. planicosta lerichei* and *C. (Arcturellina) sulcata aizyensis*) and the otolith species *Paraconger sauvagei* are statistically the same (Welsh test: $p < 0.01$), the means of the other groups are statistically different.

5.3. $\delta^{13}C$ results

In general, intra-annual variation in $\delta^{13}C$ is less consistent than in $\delta^{18}O$ (Figs. 4–6, 9; Supplement S1). The total range across all specimens extends from −5.6 to +3.9 ‰, spanning about 9.5 ‰. Within each taxon, the range in $\delta^{13}C$ is much lower, about 3 ‰ or less. Specimens of *H. solanderi* have the highest values (average of +2.8 ‰), followed by *C. (A.) sulcata* (average of +1.9 ‰), *V. planicosta lerichei* (average of +0.5 ‰) and the ophidiid otoliths (average of −1.0 ‰), with the lowest values observed in the congrid otoliths (average of −3.8 ‰). *t*-tests, or in the case of unequal variance Welsh tests, indicate that all taxon means

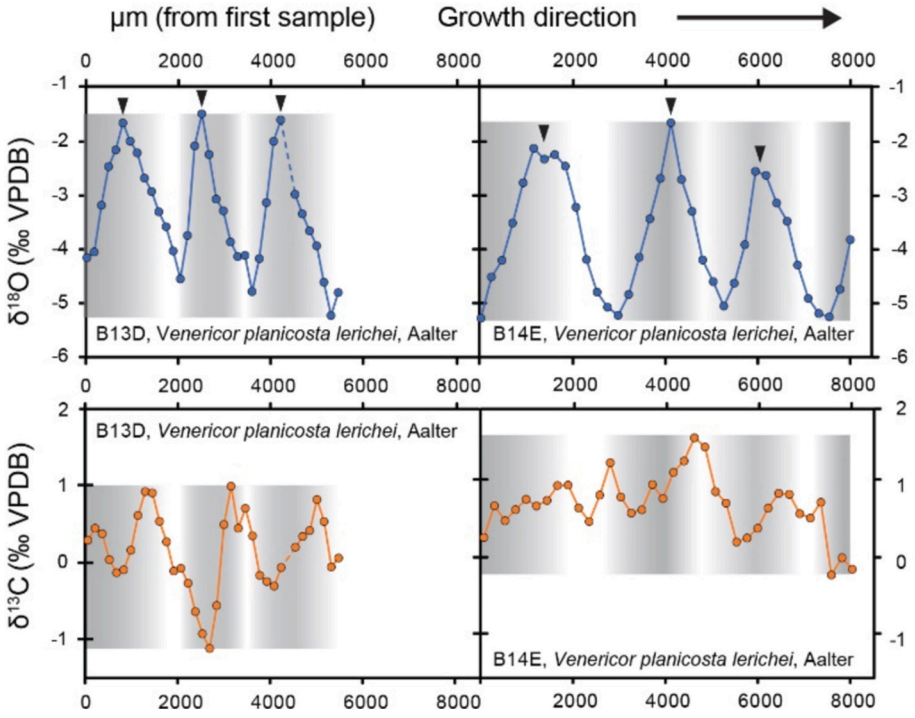

Fig. 4. $\delta^{13}C$ and $\delta^{18}Oc$ results of two serially sampled *Venericor planicosta lerichei* specimens (B13D, B14E) from the Aalter Sand Fm., Belgium. Growth increments are shown as gradient bars behind the isotope profiles. Year markers (black triangles) indicate interpreted winter peaks.

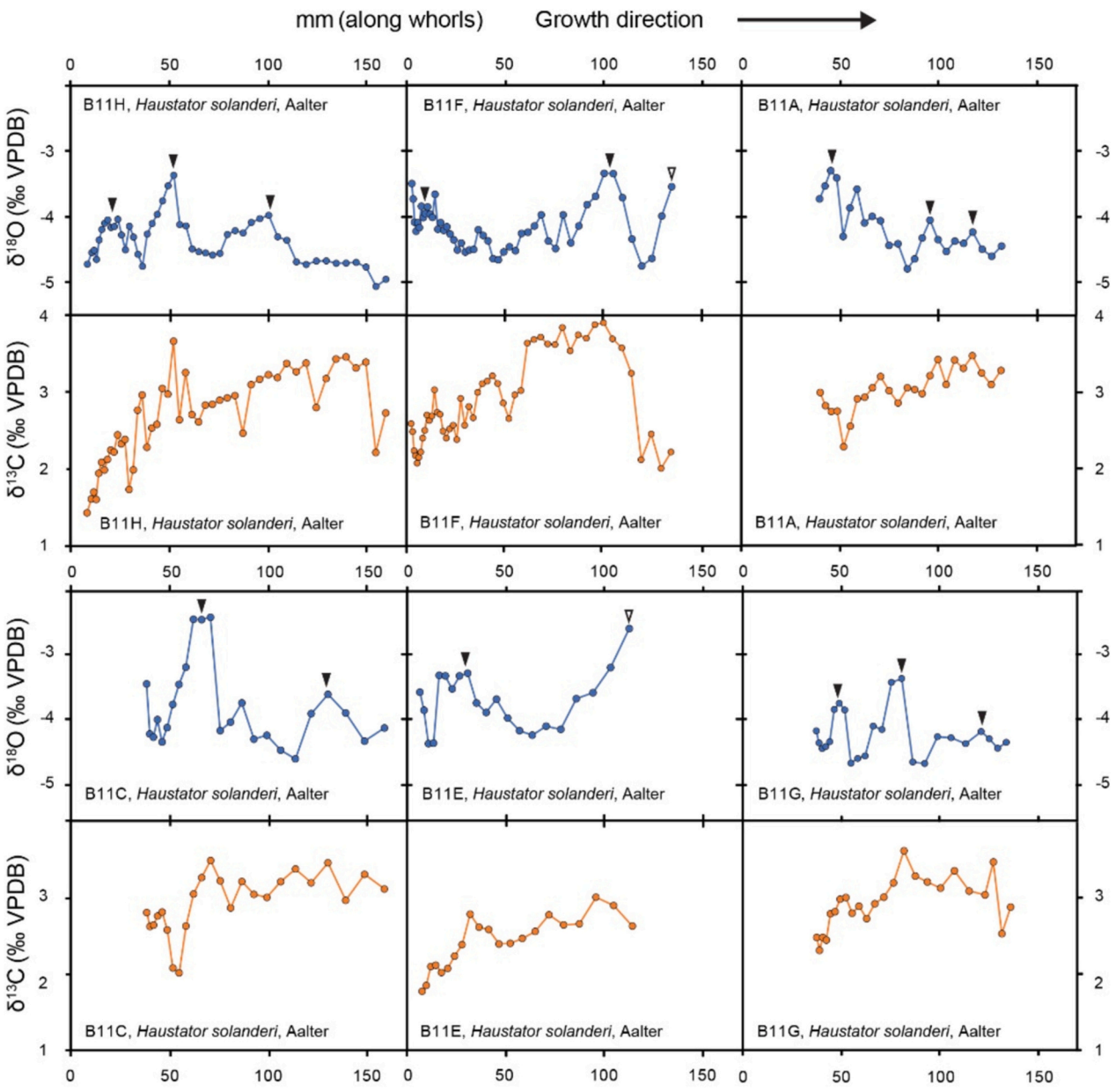

Fig. 5. $\delta^{13}C$ and $\delta^{18}Oc$ results of six serially sampled *Haustator solanderi* specimens from the Aalter Sand Fm., Belgium. Year markers (black triangles) indicate interpreted winter peaks, open triangles indicate possible winter peaks.

are statistically different. Intra-annual range of $\delta^{13}C$ is generally smallest in ophidiid otoliths from Aalter (average range of 1.0 ‰), followed by *H. solanderi* (average range of 1.6 ‰), *V. planicosta lerichei* (average range of 2.0 ‰) and congrids (average range of 2.1 ‰), whereas ophidiids from Scherpenberg show the largest average range, of 2.6 ‰. While a seasonality is apparent in the otolith $\delta^{13}C$ profiles, in particular in the congrids, intra-annual $\delta^{13}C$ variability in *H. solanderi* and *V. planicosta lerichei* does not exhibit a distinct seasonal signal. Instead, in line with previous studies on Eocene mollusks (e.g. De Winter et al., 2020; Clark et al., 2022), the $\delta^{13}C$ variability in mollusks (bivalves and gastropods) from the Aalter Sand Fm. displays significant variability within seasons and lacks a consistent pattern among the specimens. This suggests that these $\delta^{13}C$ fluctuations are not exclusively related to annual or seasonal changes in the $\delta^{13}C$ of dissolved inorganic carbon, but instead are more likely heavily influenced by fluctuating metabolic contributions of isotopically light carbon (McConnaughey and Gillikin, 2008). Notably in the turritellines, all $\delta^{13}C$ patterns show a marked increase in $\delta^{13}C$ over their life span (Fig. 5). Given that other Eocene turritelline records (Andreasson and Schmitz, 1996, 1998, 2000; Huyghe et al., 2012) show variable $\delta^{13}C$ profiles, the results from Aalter might reflect a local phenomenon.

6. Discussion

6.1. General observations

While all studied fossils from the Aalter locality should hypothetically record the same climatological conditions and environmental setting on average, their oxygen isotopic profiles show large differences, with species averages ranging from −4.1 ‰ in the turritelline gastropod *H. solanderi* to −2.5 ‰ in the ophidiid '*N.*' *subregularis*. Minimum values are comparable across *V. planicosta*, *H. solanderi*, and *P. sauvagei* and generally fall between −5.5 ‰ and − 4.5 ‰, the maximum values in these taxa range from −3.1 ‰ in *H. solanderi*, to −1.6 ‰ in *V. planicosta*, resulting in average annual ranges as large as 3.7 ‰ in *V. planicosta* to just 1.7 ‰ in *H. solanderi*. The '*N.*' *subregularis* specimens deviate in both

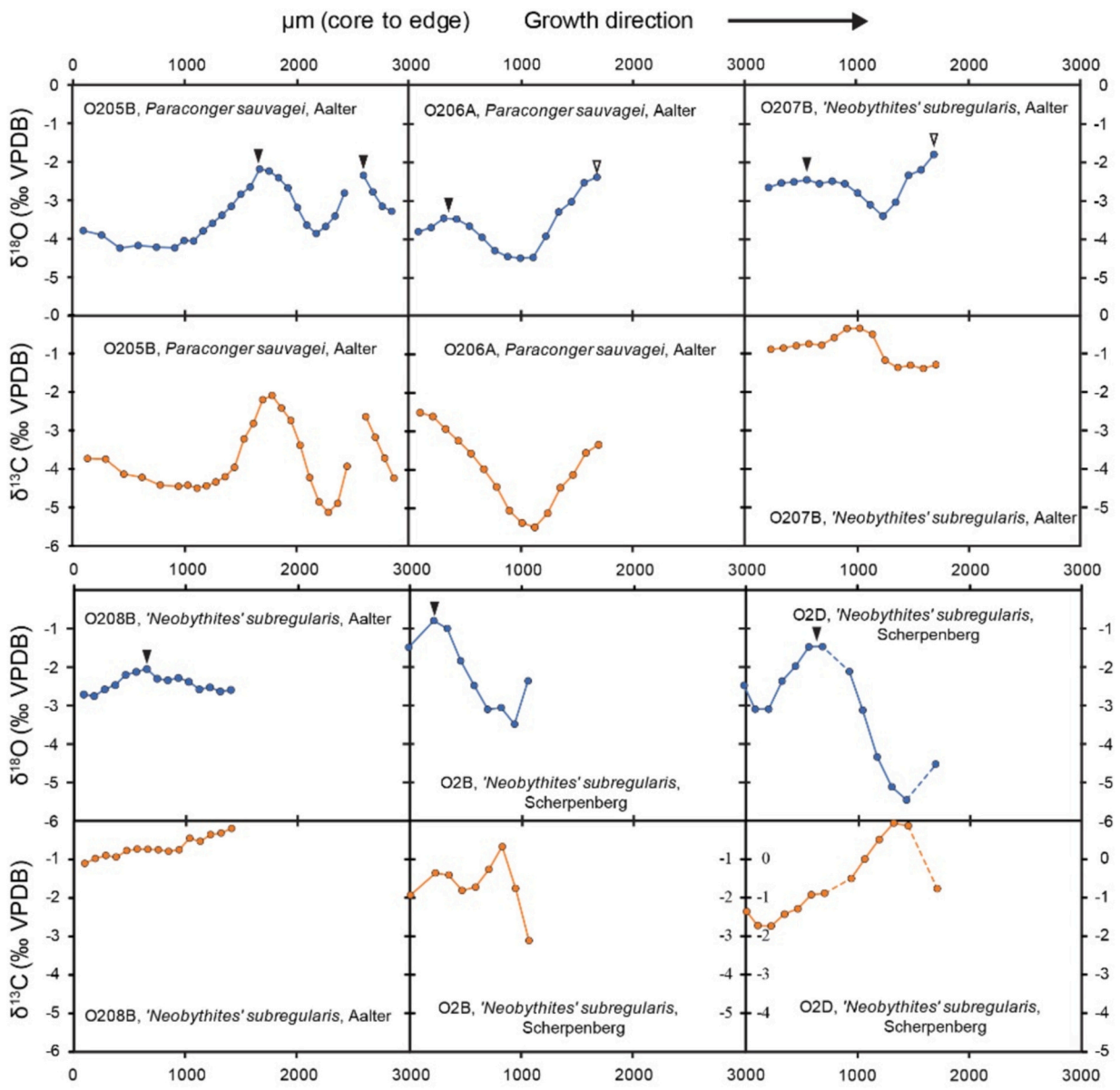

Fig. 6. $\delta^{13}C$ and $\delta^{18}Oc$ results of serially sampled *Paraconger sauvagei* (O205B, O206A) and '*Neobythites*' *subregularis* (O207B, O208B, 02B, O2D) specimens from the Aalter Sand Fm. at Aalter and Scherpenberg, Belgium. Year markers (black triangles) indicate interpreted winter peaks, open triangles indicate possible winter peaks.

minimum and maximum values, −3.4 ‰ and − 1.8 ‰, respectively (Fig. 7). The range in average specimen values (−2.3 to −4.4 ‰), statistical difference between most taxon means, and variability in specimen ranges could mean that organisms recorded different conditions during their lifetimes, or over the period of time covered by the death assemblage in which they occur, or that mineralization did not occur in equilibrium for some of the taxa. Potential disequilibrium mineralization is difficult to assess with conventional isotopes for fossil taxa, as ancient water composition is not availible. Nevertheless, for oxygen isotopes at least, there is little indication that mollusks today precipitate carbonate significantly out of equilibrium with seawater (Wefer and Berger, 1991; Immenhauser et al., 2016). Specifically for *V. planicosta,* it has recently been argued based on dual clumped isotopes that mineralization occurred in equilibrium (Kniest et al., 2024). If this also is the case for the other analyzed taxa, organisms preserved in the Aalter coquina beds must have precipitated carbonate in waters of different isotopic composition, temperature, or a combination of both. In this and the subsequent sections, we explore the ecological, paleoenvironmental and taphonomical factors that likely contribute to the observed variability in intra-annual and average $\delta^{18}O$ recorded by the different taxa from the coquinas.

6.2. Taphonomy

Both coquinas are assumed to have been deposited within a relatively short time interval, probably within hundreds to thousands of years each. The overall good preservation of the fossil assemblage is consistent with relatively rapid burial below the taphonomically active zone. Nevertheless, because coquina beds are concentrations of shells, likely accumulated on the bottoms of subtidal channels and winnowed by currents or storms, they likely represent an amalgamation of material transported from various local microhabitats or nearby environments over some number of years. The complex depositional setting of the Oedelem Member, with lagoons or mudflats likely nearby and potentially variable salinity, makes some degree of environmental averaging likely, which could account for the isotopic variation seen among our samples. In addition to spatial variation, true climate variability happening on a time scale shorter than shell-bed formation could well be

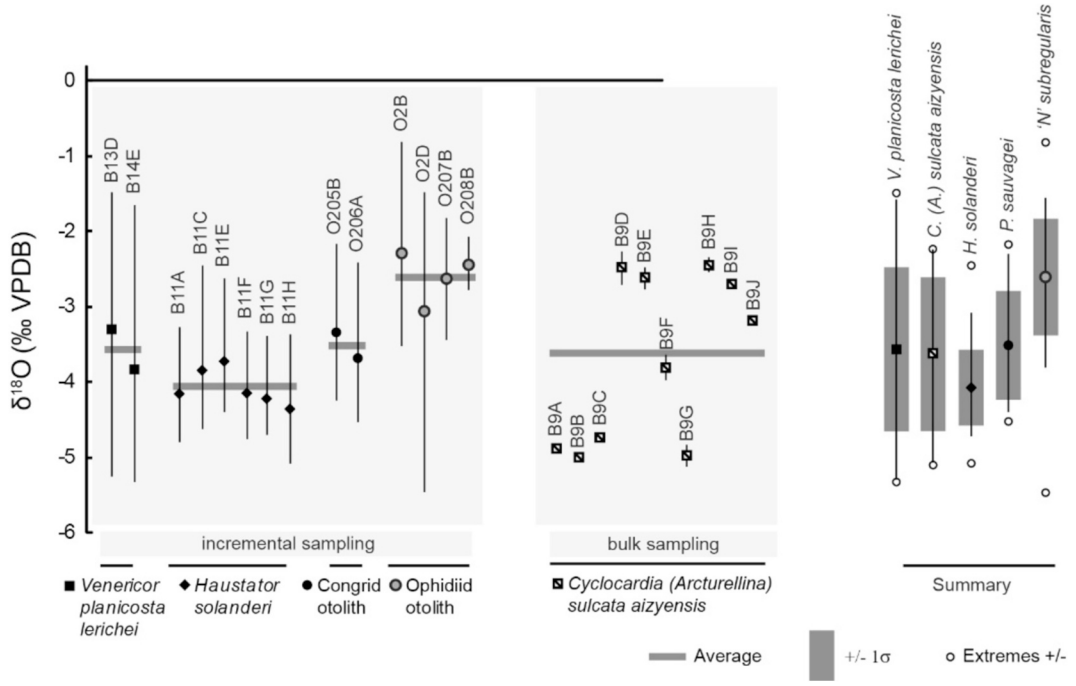

Fig. 7. δ^{18}Oc ranges for all sampled specimens of the Aalter Sand Fm. at Aalter and Scherpenberg, Belgium. Average and maximum range of individual specimens are shown on the left, and summaries for each taxon (average, standard deviation, average minima and maxima, extremes) on the right.

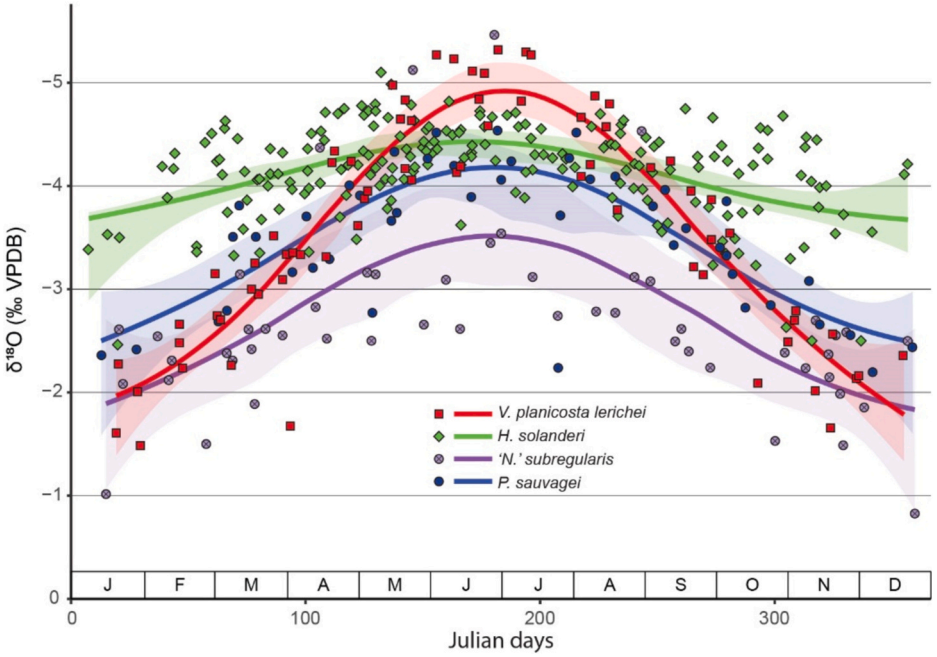

Fig. 8. Mean annual cycles for each taxon generated by ShellChron 0.4.0 using δ^{18}Oc data for *H. solanderi*, *V. planicosta*, *P. sauvagei* and '*N.*' *subregularis*. Lines represent a sinusoidal regression curve generated based on the data of each species. Ribbons represent the 95 % confidence intervals of the different species. Letters J-D represent months.

responsible for differences in average and intra-annual range in δ^{18}O between individual specimens. While the studied interval covers a time period with less severe climate events than during the preceding EECO (which comprises major hyperthermals such as Eocene Thermal Maximum 2 and Eocene Thermal Maximum 3), at least one smaller hyperthermal event has been recorded between 49.4 Ma and 49.0 Ma (event "C22nH4" in Westerhold et al., 2018). It is therefore not unconceivable that part of the isotopic differences recorded between different specimens and species within these coquinas actually represents short-term climate variation captured within the death assemblage represented by the studied coquinas.

Not all studied fossil groups are likely to have been transported to the same degree. In general, the good preservation of the turritellines and carditids argues in favor of limited reworking or transport. *Venericor planicosta lerichei* shells are heavy and large (6–10 cm length) in comparison with the more lightly built turritelline shells (3.5 cm height),

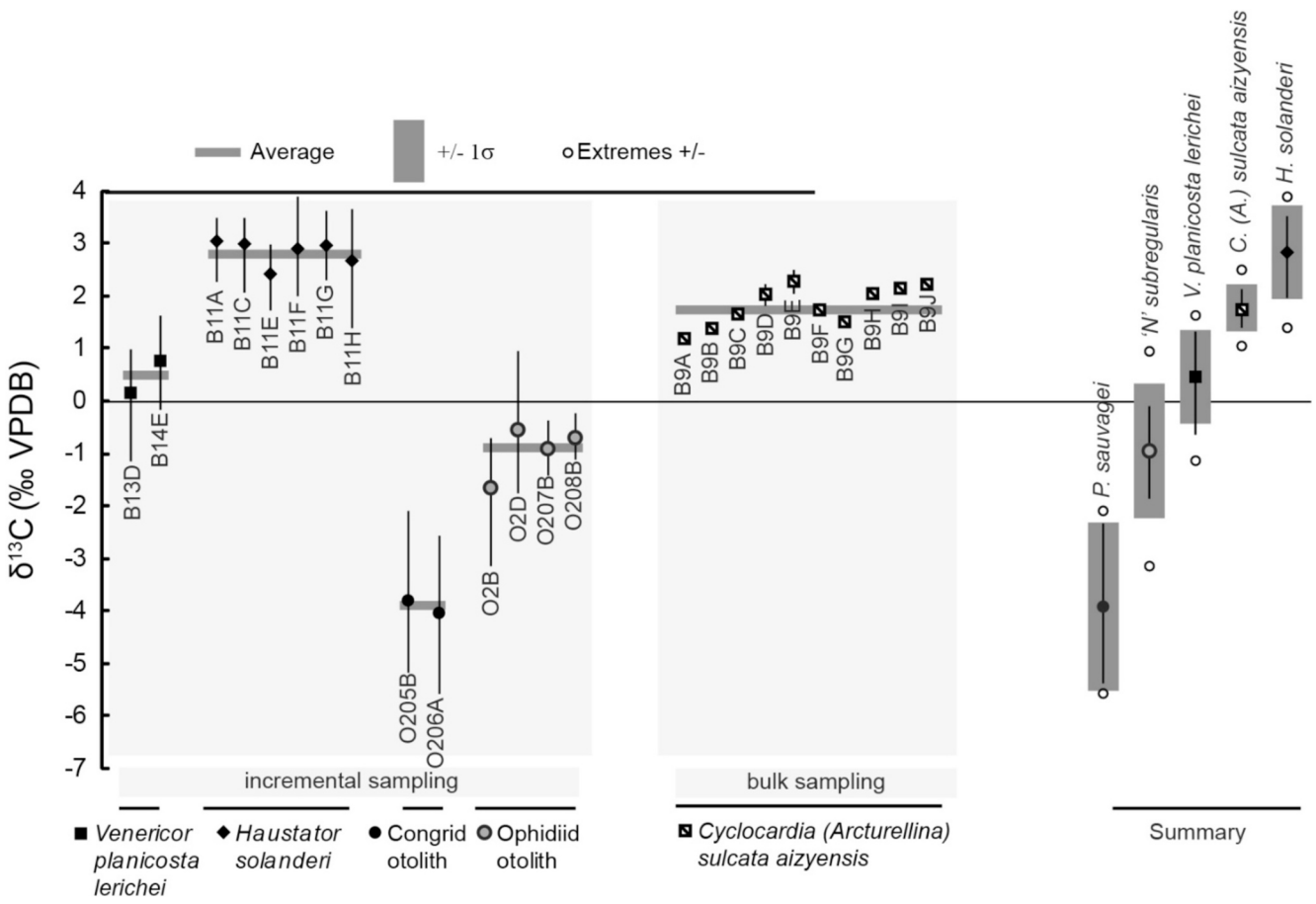

Fig. 9. $\delta^{13}C$ ranges for all sampled specimens of the Aalter Sand Fm. in Aalter and Scherpenberg, Belgium. Average and maximum specimen range of individual specimens are shown on the left, and summaries for each taxon (average, standard deviation, average minima and maxima, extremes) on the right.

small carditids (*Cyclocardia*; <1 cm length) and otoliths (3–5 mm length), suggesting a generally lower post-mortem transportability. Sessa et al. (2012) found higher isotopic variability among small venericards in the early Eocene of the US Gulf Coast in comparison with large co-occurring specimens, and they suggested transportation of smaller shells as well. Notably, articulated valves of *V. planicosta* occur towards the top of the venericard coquina in Aalter, suggesting rapid burial without major transportation (Steurbaut and Nolf, 1989).

Similar to the venericards, the turritelline shells are largely intact and mostly devoid of epibionts, arguing against endured transport or exposure at the surface. They are nonetheless slightly worn, probably due to low-energy winnowing in the subtidal distribution channels (Jacobs, 2015). Supply of specimens to the winnowing site by storm events cannot be ruled out, since the coquinas were deposited above the storm wave base. As some modern turritellines are known to also live on tidal flats and low tide beaches (Waite and Allmon, 2013), it is possible that the *H. solanderi* shells were transported to the subtidal channels from local nearby mudflats post mortem. This could have resulted in their oxygen isotopic profiles deviating from *V. planicosta*, which is considered to have lived strictly in the subtidal environment represented by the Oedelem Mbr.

The otoliths are the smallest fossils studied (3–5 mm length) and are therefore the most prone to post-mortem sedimentary transport. As such, their isotopic composition o could reflect conditions across a range of nearby environments, including those beyond what was occupied by the turritellines and venericards. On top of this, a major principle in otolith taphonomy is the actualistic observation that otoliths are not digested by predators, but accumulate in their intestines or are excreted (Nolf, 1985, 1995). The majority of otoliths arriving in a typical thanatocoenosis are in fact delivered as the excretion products of free-swimming predatory fish such as sharks, many of which can migrate over considerable distances. This provides a mechanism through which otoliths from different habitats can be delivered to the subtidal environment where turritellines and carditids live (Nolf, 1995; Vanhove et al., 2012). Importation from deeper, cooler environments could explain the more positive average $\delta^{18}O$ values of the ophidiid otoliths compared to congrid otoliths, turritellines and carditids. In addition, marked differences in the mean and range of the oxygen isotope profiles of ophidiid specimens between the Scherpenberg and Alter localities could reflect differences in proximity to deeper hunting grounds for predatory fish…

Taken together, and given the complexities involved in the deposition of coquina beds, it appears likely that the otolith isotope records reflect environmental conditions over a wider range of habitats and environments than the other taxa (Fig. 10), due to a combination of sediment transport and *syn*-postmortem transport by free-swimming predatory fish. The turritellines could have been transported over short distances, reflecting local environmental heterogeneity, while the large venericards experienced only local winnowing and were not transported over considerable distances at all.

6.3. Paleobiology and -ecology

On top of these depositional and taphonomic processes, the paleobiology and ecology of the studied species played a role in the observed isotopic discrepancies as well. Mobility is particularly relevant here, as is habitat breadth. More mobile taxa may escape to more favorable habitats during some parts of the year, or parts of their life cycle. If they

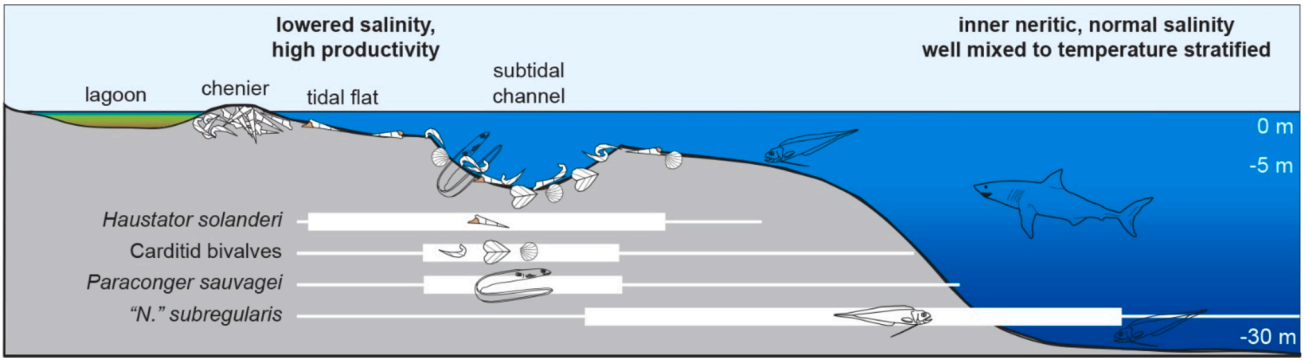

Fig. 10. Simplified paleoenvironmental reconstruction of the coquina layers in the Aalter Sand Fm. and estimated habitat ranges of the organisms used in this study based on species stable isotopes.

encountered different environmental settings over their life span, such as deeper water or river mouths, this could introduce additional variability in their isotope profiles.

Among the studied species, carditid bivalves are generally lethargic and move only slowly and infrequently (Yonge, 1969), living just below the surface of the sediment. We therefore consider them most likely to record in situ intra-annual variation in temperature and/or water composition.

Turritellines live partly buried in sediments with the aperture exposed for filter feeding. Nevertheless, active movement on the substrate has also been observed and is probably an underestimated characteristic of turritelline behavior (Allmon, 2011). Turritellines are generally considered typical of a subtidal environment (Dominici and Kowalke, 2014). Nevertheless, based on $\delta^{13}C$ values and size distribution of *Turritella leucostoma* on the San Felipe tidal flat, where only adults were observed, it was suggested that planktonic larvae of this species settle in deeper settings, while adults move towards more proximal tidal channels and low tide beaches (Allmon, 1988, 2011; Waite and Allmon, 2013), migrating over several hundreds of meters during their adult lives. The potential for mobility could explain the variability in turritelline stable oxygen isotope profiles, showing less consistent annual cyclicity than the more sedentary carditid bivalves.

Among the fishes, *Paraconger* is known to live predominantly buried in the substrate with only the head exposed, without migrating large distances (Smith, 1989; FishBase, 2023). The otoliths of this species therefore likely primarily record in situ conditions (e.g. Ivany et al., 2000). Indeed, the taxon mean of *P. sauvagei* from Aalter is statistically indistinguishable from those of the two species of carditid bivalves (*V. planicosta lerichei* and *C. (Arcturellina) sulcata aizyensis*; Welsh test: $p < 0.01$), the least mobile of the studied taxa. The benthopelagic ophidiid '*N.*' *subregularis*, in contrast, was likely more vagile (FishBase, 2023), and ophidiids today are found over a great range of depths (neritic to bathyal; Vanhove et al., 2012; FishBase, 2023), and so otoliths from this taxon could collectively record conditions over a wider spectrum of habitats before coming to rest in the Aalter Sand Fm.

When comparing the isotope profiles of the carditid bivalves, the turritelline gastropods and the congrid fishes, i.e. the taxa that are interpreted to reflect the more local environment, it is notable that, while the average of the 5 % minimum values differ by less than 0.8 ‰, the average of the 5 % maximum values differ up to 1.4 ‰ among these taxa (Fig. 8). This difference is most pronounced between the turritelline gastropods and the other taxa. It is possible that the turritellines lived in more proximal settings, somewhat more depleted in winter than the site where the carditids lived and were transported syn/post-mortem to accumulate in tidal channels. Alternatively, in summer, more mobile taxa like the turritelline gastropods could migrate to deeper waters to escape the thermal stress characteristic of intertidal environments (Dong et al., 2022), reducing their seasonal isotopic range. Nonetheless, it is questionable whether the very shallow depth gradient in the Belgian part of the sNSB (Jacobs et al., 1991; Jacobs and Sevens, 1993; Vandenberghe et al., 2004) could account for sufficient local depth differences to result in lateral temperature or $\delta^{18}O_{sw}$ variability large enough to result in isotopic differences of up to 1.4 ‰, without invoking significant freshwater input or evaporative conditions. Both evaporative conditions and the significant input of isotopically light freshwater are deemed unlikely, considering the normal salinity conditions indicated by the fauna of the Aalter Fm.

Variability in mean and range among taxa could also be caused by differences in growth rates through the year, with on season or another not fully captured by carbonate accretion depending on the taxon. Variation in growth rate and shutdown of growth under certain conditions, during reproduction or in function of their life span, is frequently documented in modern and fossil mollusks and even otoliths (many authors, including Wurster and Patterson, 2001; Pilling et al., 2007; Ullmann et al., 2010; e.g. Versteegh et al., 2010; Schwartzmann et al., 2011; Strauss et al., 2014; De Winter et al., 2018). If growth rate reduced significantly during winter, e.g., this season will be less represented in the secreted carbonate, resulting in biased specimen and taxon averages and ranges. Potentially, the isotope profile of *V. planicosta*, which encompasses the largest seasonal isotope range, represents the full seasonal cycle, while the isotope profiles of the turritelline gastropods and congrid otoliths only represent part of the seasonal cycle in temperature and sea water isotopic composition.

Unfortunately, rate of growth and growth cessation are difficult to assess in fossil specimens, but the shape of the isotope profiles can provide some clues (e.g. Goodwin et al., 2003; Ivany, 2012; Judd et al., 2018; De Winter, 2022). Macroscopic growth increments in our two *V. planicosta* shells co-vary with isotope data, suggesting that the growth banding in venericards is annual. Even though sampling resolution should be high enough to resolve (quasi)sinusoidal annual cycles (>10 samples per annual cycle), most peaks are saw-toothed. Slower growth in winter months has been inferred from cuspate $\delta^{18}O$ profiles in fossil venericards from the Eocene, in several previous studies (Andreasson and Schmitz, 1996; Purton and Brasier, 1999; Kobashi et al., 2001). Therefore, although the *V. planicosta* shells might represent the most complete seasonal cycle among the studied taxa, actual $\delta^{18}O$ variation could have been even larger. Consequently, the intra-annual ranges recorded in our specimens should be seen as minimum estimates.

Intra-annual $\delta^{18}O$ variations of the turritelline specimens are less straightforward to interpret. Cycles vary in shape and amplitude, potentially resulting from the more mobile behavior of the turritellines. The results from the ShellChron model reveal considerable variations in growth rate throughout the lives of the studied specimens, ranging from >1000 μm/day during growth peaks, to as little as <10 μm/day during winter growth breaks. In several of the studied specimens (e.g. in B11C, B11H, B11G) some of the winter peaks are sharp and appear to be truncated, suggesting that time is missing and sampling resolution was not high enough across the increments secreted in winters to capture the

full seasonal range. Previous studies (e.g. Anderson and Allmon, 2020) have suggested that growth is particularly fast in the first year, followed by a decline in growth rate in subsequent years. While not immediately evident from the results of this study, a decrease in growth rate with age would mean that subsequent years require increasingly high sampling resolution to capture the full seasonal cycle.

The oxygen isotopic profiles of the otoliths of *P. sauvagei* also show a distinct cuspate profile, indicating slower growth, or even growth cessation, in winter months. The profiles of '*N.*' *subregularis* show less consistent patterns between the specimens. Given that the otolith records from this species generally represent less than one full year, it is difficult to assess patterns of growth in these otoliths. Indeed, in organisms that have very short lifespans, the isotopic means and ranges could be biased, because of incomplete annual cycles.

These observations highlight that life history traits can introduce additional complexity in interpreting sclerochronological isotope profiles. Intra-annual records of short-lived species are potentially incomplete and should be interpreted with extra care. A very short life span might also explain the relatively large range in whole-shell $\delta^{18}O$ values between the different *Cyclocardia* shells. To our knowledge, no information is available about the biology, life span or variability in growth rate in this genus. Hence, these small mollusks may be short-lived and different individuals may have had different spawning seasons, thus their shell values represent seasonally biased temperatures instead of true mean annual conditions. Further study would be needed to confirm this.

Of the fish otoliths, the *Paraconger* genus is known to grow older than '*Neobythites*' (Ivany et al., 2003; Vanhove et al., 2011), which is confirmed here based on the shape of the $\delta^{18}O$ profiles, with an estimated lifespan for *P. sauvagei* of up to 2 years, compared to up to one year for '*N.*' *subregularis*. This suggest that intra-annual stable isotope records of *P. sauvagei* are better suited to reconstruct seasonality.

Lifespans of turritellines derived from $\delta^{18}O$ profiles of various modern and fossil species rarely exceed 5 years, with most growth taking place during the first year, followed by a drastic decline in growth rate during the subsequent years (Allmon et al., 1992; Jones and Allmon, 1995; Andreasson and Schmitz, 1996; Jones, 1998; Teusch et al., 2002; Latal et al., 2006; Allmon, 2011; Anderson and Allmon, 2020; Ivany et al., 2018). Our results are in line with a relatively short lifespan for turritellines. The $\delta^{18}O$ profiles of the *H. solanderi* specimens yield estimate ages ranging between 1 and 3.5 years, suggesting that this species lived no more than about 4 years.

Even though we only sampled three years of our *Venericor* specimens for stable isotope analyses, macroscopic growth increments indicate lifespans of 9–13 years for the studied specimens. This is in line with previous studies, which demonstrate lifespans of various *Venericardia* species ranging from 10 to 30 years (Ivany et al., 2004, 2018). Hence, *V. planicosta* has the longest life span of the studied taxa. In combination with their lethargic behavior and consistent seasonal isotopic signal, *Venericor* likely represents the most reliable of the different types of archives studied here, in terms of recording environmental conditions at the Aalter paleoenvironment.

6.4. Implications for seasonality in the sNSB

The isotopic profile of *V. planicosta* shells from Aalter show a seasonal range in $\delta^{18}O_{carbonate}$ between −1.5 and − 5.3 ‰, reflecting a considerable seasonality in temperature and/or sea water composition. When one would assume a constant sea water oxygen isotopic composition ($\delta^{18}O_w$) throughout the year, a seasonal temperature range could be calculated. For paleotemperature calculations based on stable oxygen isotopes of aragonitic mollusks, we apply the equation of Grossman and Ku (1986) using a modified version in which $\delta^{18}O_w$ is cast in VSMOW instead of PDB (Goodwin et al., 2001). Given that $\delta^{18}O_w$ is not constrained for the Aalter environment, determining absolute summer and winter temperatures is difficult. While the global average $\delta^{18}O_w$ of the ice-free early Eocene world will have been around ~ −1 ‰ (Zachos et al., 1994; Roberts et al., 2009), water isotope-enabled general circulation models suggest that the partly enclosed early Eocene sNSB region might have been characterized by slightly more depleted waters, of up to −2 ‰ (Tindall et al., 2010; Zhu et al., 2020). With this estimated $\delta^{18}O_w$, calculated sea water temperatures would correspond to an annual range of 18 to 34 °C, compared to previously reconstructed mean annual bottom water temperatures of 27–31 °C for the mid to late Ypresian sNSB using Mg/Ca and clumped isotopes on large benthic foraminifera (Evans et al., 2018; Martens et al., 2022).

If the sea water oxygen isotopic composition was constant throughout the year, the intra-annual range of 3.8 ‰ in *V. planicosta* would imply a range in seasonal water temperatures of ~16 °C. This is considerably larger than the modern global average seasonal sea surface temperature range of 8–9 °C at 41°N (Ivany, 2012). It is also larger than present-day ranges in the sNSB of about 10–12 °C in a well-mixed water column (Andreasson and Schmitz, 2000; Austin et al., 2006). We therefore consider it possible that the Aalter region was characterized by some seasonal variation in seawater oxygen isotopic composition. Relatively more depleted waters in summer and/or more enriched waters in winter could account for the relatively large seasonal range recorded in $\delta^{18}O_{carbonate}$, similar to the conditions in the Paris Basin during the Middle Eocene Climatic Optimum (40 Ma; Kniest et al., 2024). Nonetheless, the sedimentology and paleontology of the Aalter succession suggests that the depositional environment was generally characterized by fully marine conditions under normal salinity, limiting possible seasonal salinity variations. Future studies using clumped isotope thermometry would allow us to separate the effects of temperature and seawater isotopic composition on the oxygen isotope composition of carbonates (Eiler, 2007; De Winter et al., 2022; Meckler et al., 2022; Keating-Bitonti et al., 2011; De Winter et al., 2024; Kniest et al., 2024), enabling us to constrain the absolute seasonal variability temperature and/or sea water composition during the deposition of the Aalter Sand Formation.

6.5. Causes for variability in $\delta^{13}C$

In our dataset, the taxon means of $\delta^{13}C$ values range between −3.9 ‰ (congrid otoliths) and + 2.8 ‰ (turritellines), with little overlap between the ranges of the taxa (Fig. 9). The relative sequence of the offsets – turritellines with the highest values, followed by venericards, ophidiids, and finally congrids – is consistent with most of the limited data available for comparison in literature (e.g. Andreasson and Schmitz, 1996; Ivany et al., 2003; Kobashi et al., 2004; Vanhove et al., 2012; Huyghe et al., 2012).

Unraveling the causes of $\delta^{13}C$ variations in biogenic carbonates is considerably more complex than interpreting $\delta^{18}O$ profiles (Wefer and Berger, 1991; McConnaughey and Gillikin, 2008). Variations are controlled by the relative contributions of respired (R) and environmental DIC (1-R) and their $\delta^{13}C$ values. While continental freshwater input of isotopically negative environmental DIC is one of the main causes of carbon isotopic variability in biological records from coastal environments (McConnaughey and Gillikin, 2008), sedimentological and paleontological evidence suggests that freshwater input was limited in the Aalter depositional environment. The fraction of respired DIC (R) incorporated into biogenic carbonate varies between species and over lifespans as a function of metabolic growth rate (Schwarcz et al., 1998; McConnaughey and Gillikin, 2008), and the isotopic value or respired DIC varies with trophic level (Peterson and Fry, 1987). The fraction of respired DIC in shell material is also dependent upon the locus of precipitation within the shell, with the inner shell layer tending to be more depleted in ^{13}C than the outer (Ivany et al., 2008). In general, reported R values for modern mollusks are 10 % or less, while those for fish are higher, up to 40 % (Gillikin et al., 2006; Solomon et al., 2006; McConnaughey and Gillikin, 2008; Tohse and Mugiya, 2008; Lartaud et al., 2010). As respired DIC is considerably more depleted than that of

ambient seawater (McConnaughey and Gillikin, 2008), a difference in R is a likely explanation for why values of turritellines and venericards are enriched compared to congrids and ophidiids. The marked increase in $\delta^{13}C$ over the life span of the turritellines (Fig. 5) could be compatible with an ontogenetic decrease in respired DIC contribution, or a change in habitat through their lives (Van Horebeek et al., 2021). Concerning the otoliths, congrids and ophidiids feed at approximately the same trophic level, on plankton and small benthic prey, including annelid worms, crustaceans, and small fish (Takai et al., 2002; FishBase, 2023), which all have tissue $\delta^{13}C$ compositions of around −15 ‰ (Takai et al., 2002). Nevertheless, congrid otolith $\delta^{13}C$ is considerably more depleted than ophidiid otolith $\delta^{13}C$. If these fish taxa indeed occupied different habitats, as inferred based on their $\delta^{18}O$ data, the $\delta^{13}C$ offset would support of a more distal habitat for ophidiids, since their $\delta^{13}C$ are closer to $\delta^{13}C$ of open marine DIC.

6.6. Comparison with the Egem Member fauna

While only few sclerochronological studies have been performed on the late Ypresian sNSB, the records from the nearby upper middle Ypresian Egem Mb. (Vanhove et al., 2012) provide an interesting comparison. There, similar taxa were analyzed, including otoliths of the congrid *Paraconger papointi* and the ophidiid '*N.*' *subregularis*, and the bivalve *Cyclocardia (Arcturellina) sulcata* (Vanhove et al., 2012). The Egem Mb. was sampled in the Ampe Clay Pit, located 17 km SW of Aalter. It comprises nearshore to shore-face sand deposits, deposited within the EECO interval, about 2 myr before the deposition of the Aalter Fm. (Vandenberghe et al., 2004; Steurbaut, 2015).

A cross-plot of specimen averages of $\delta^{13}C$ and $\delta^{18}O$ data (Fig. 11) reveals consistency between the upper Ypresian Aalter Fm. (this study) and the upper middle Ypresian Egem Mb. (Vanhove et al., 2012). Results from similar taxa show at least partial overlap in both isotopes. In both the Aalter Fm. and Egem Mb., taxa plot as distinct groups, primarily due to the distinct taxon-specific $\delta^{13}C$ signatures of each taxon. In both units, the mean of the specimen averages in $\delta^{18}O$ of ophidiids is the most positive of all taxa, corroborating that ophidiids indeed seem to record a different ambient condition compared to the other taxa. For both ophidiids and congrids, the Egem Mb. specimens show a wider spread in $\delta^{18}O$ values, possibly related to the more proximal setting of the Egem Mb. Sands (Steurbaut, 2006; Martens et al., 2022), resulting in larger variability in temperature and salinity. A rather significant difference between the lithostratigraphic units is that the range of the averages of *C. (A.) sulcata aizyensis* from the Aalter Fm. is about double that of *C. (A.) sulcata* from the Egem Mb. While the reason remains unclear, it should be reiterated that the size of this taxon is very small and little is known about their life span. The cross-plot demonstrates that by measuring multiple taxa and multiple specimens in a stratigraphic unit, the observed isotopic variation becomes more representative of the total range of isotopic variation of its macrofauna. Only by measuring multiple taxa can one obtain an understanding of the extent to which the different taxa capture the full seasonality.

7. Conclusions and recommendations

Our work has implications for studies reconstructing intra-annual trends in paleotemperature and seasonality based on skeletal archives from shallow marine settings. Based on the results of this study, several recommendations can be made for future sclerochronological studies focusing on multitaxon assemblages:

(1) In general, it is crucial to assess the sedimentological and taphonomic processes involved in the deposition of the sedimentary record and fossils within. Many macrofossil-rich deposits are the result of winnowing or transport, causing time averaging within the death assemblage and possibly introducing elements from a variety of different local microhabitats into the assemblage. The

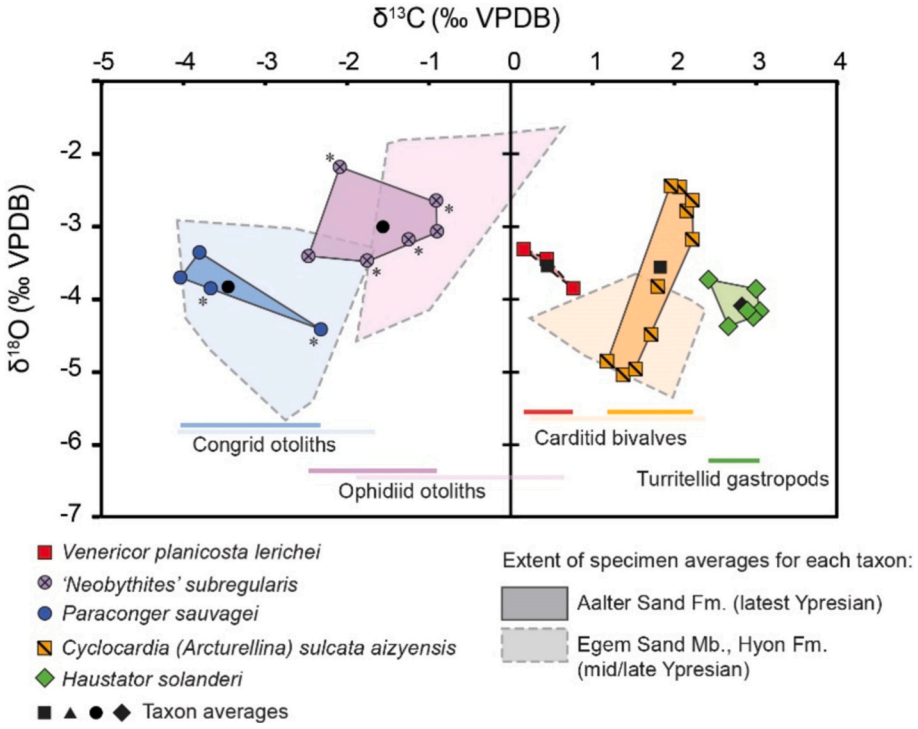

Fig. 11. Cross-plot of specimen average $\delta^{18}Oc$ and $\delta^{13}C$ values of congrid and ophidiid otoliths, carditid bivalves and turritelline gastropods, based on bulk sampling (bulk line samples or ground whole specimens) or averages of serially sampled data. Specimens marked by an asterisk are from Vanhove et al. (2011). Light grey fields are taxon extents from the inner neritic Egem locality of mid to late Ypresian age (~51 Ma), located 18 km SW of Aalter (Vanhove et al., 2012). The cross-plot shows overall resemblance between both shallow marine sites in the position of otoliths and bivalves on the cross-plot. Taxa can be distinguished from each other on the cross-plot due to the taxon-specific differences in δ13C.

least transported fossils, such as bivalves preserved in live position, will yield the most consistent and representative data. Moreover, the largest fossils are least likely to be transported. Smaller fossils, such as fish otoliths, are more likely to have undergone some transport, both sedimentary as well as intestinal by predatory fish. Otolith isotope records could therefore reflect environmental conditions over a wider range of habitats and environments in comparison to mollusks.

(2) When selecting incrementally mineralized fossils as short-term archives of past climate, the least mobile or most lethargic animals are to be preferred. More motile animals, such as gastropods and fish, can introduce additional variability in their isotope profiles, as they could reflect a wider range of habitats and environments. Among non-migratory groundfish, congrids likely reflect a more local signal than ophidiids, because they are known to live predominantly buried in the substrate, with only the head exposed, while ophidiids are more vagile benthopelagic fish.

(3) Overall, species with lifespans of several years provide more robust records of seasonality, compared to species with very short lifespans, as longer-lived species can provide a multi-year record of seasonality, accommodating year-to-year variability. In this respect, large bivalves, gastropods and congrids generally capture more than one full seasonal cycle. The Paleogene ophidiids from the sNSB, on the other hand, appear to be generally short-lived, hampering accurate assessment of seasonality, unless a large number of individuals are sampled. At the same time, short-lived species often show faster growth rates, potentially providing higher resolution records, indicating a trade-of between longevity and resolution.

(4) Variation in growth rate and shutdown of growth under certain ambient conditions, during particular seasons, or over ontogeny, has been documented both in fossil mollusks and otoliths, leading to an incomplete representation of the seasonal cycle in their growth increments. In our Paleogene records, congrids, ophidiids and turritellines each show considerable slowdown in growth in parts or their record, possibly not fully capturing the seasonal cycle. Of the studied fossil groups, carditid bivalves appear to record the most complete representation of seasonal cycles. However, the saw-toothed pattern of their isotope profiles suggests that growth slowdowns likely occur and that the intra-annual ranges recorded in carditid bivalves should be seen as minimum estimates.

(5) In a dynamic coastal environment, accumulation of organisms with different habitat preferences and niches into one thanatocoenosis implies that environmental parameters derived from one taxonomic group, or only one specimen for each taxon, cannot be representative for the isotopic variability in this death assemblage and environment. Examination of multiple individual specimens spanning several different taxonomic groups considerably increases the likelihood of capturing the full range of isotopic variation of the environment.

(6) After selecting the most suitable incrementally mineralized fossils, separating the effects of temperature and sea water isotopic composition on the oxygen isotope composition of carbonates can nonetheless be difficult. Application of additional tools (e.g. seasonally resolved crumpled isotopes) may be necessary to allow reconstruction of the absolute seasonal variability in temperature and sea water composition.

Author contributions

JV, DV, ES and RPS conceived the research. DV performed stable isotope analyses. IJ performed ShellChron modelling. PC and LCI provided guidance in stable isotope laboratories. JV and DV wrote the manuscript text; NJDW revised the manuscript text critically.

Credit authorship contribution statement

Johan Vellekoop: Writing – review & editing, Writing – original draft, Visualization, Project administration, Conceptualization. **Daan Vanhove:** Writing – original draft, Project administration, Methodology, Investigation, Formal analysis, Data curation, Conceptualization. **Inge Jelu:** Software, Methodology, Formal analysis. **Philippe Claeys:** Supervision. **Linda C. Ivany:** Supervision. **Niels J. de Winter:** Writing – original draft. **Robert P. Speijer:** Writing – review & editing, Supervision. **Etienne Steurbaut:** Writing – review & editing, Supervision.

Declaration of competing interest

The authors declare that they have no conflict of interest.

Data availability

All stable isotope data generated are provided in Supplement S1.

Acknowledgements

Annelise Folie is thanked for providing access to the INS collections and permission for destructive analyses on loaned specimens of *V. planicosta lerichei*. We are grateful to Peter Stassen for his help with SEM imaging, and Rieko Adriaens for his help with XRD analyses. We thank Herman Nijs, David K. Moss, Lora Wingate and Michael Korntheuer who assisted with sample preparation or stable isotope analysis. This research was funded by the Belgian Federal Science Policy (BELSPO) through FED-tWIN project Prf-2020-038 (MicroPAST), through KU Leuven STG grant 3E211203 to J.V., through a grant by the Agency for Innovation through Science and Technology to D.V. (IWT SB093015) and grants by the Research Foundation Flanders (FWO) to R.P·S, P.C. and E.S. (G.0422.10 N) and N.J.W. (12ZB220N; Scientific Prize Climate Research). PC thanks FWO Hercules foundation and VUB Strategic Research for support of Stable Isotope Lab. LCI was supported in part by EAR-0719645 from the US National Science Foundation.

Declaration of interests

The authors declare that they have no known competing financial interests or personal relationships that could have appeared to influence the work reported in this paper.

Appendix A. Appendices

A.1. Appendix A. Description of the turritelline and otolith sampling in Aalter, Belgium: V324 ("Aalter Hagepreekstraat")

Date: 01 November 2010.
Coordinates (degrees): 51°05′8.51“ N 003°27’5.45” E
Address: Hagepreekstraat, Aalter, Belgium
Construction pit for apartment building, samples taken from excavated sands.
Constructor: Mevaco, Durmelaan 6, Aalter.

2.5–3 m thick profile visible:

- Sand stone layer of 0.25 m thick about 0.8 m below surface, disappears towards the southwest.
- Below stone layer: 2.5 m brown to green medium sand with shell coquinas, decalcified towards the southwest.

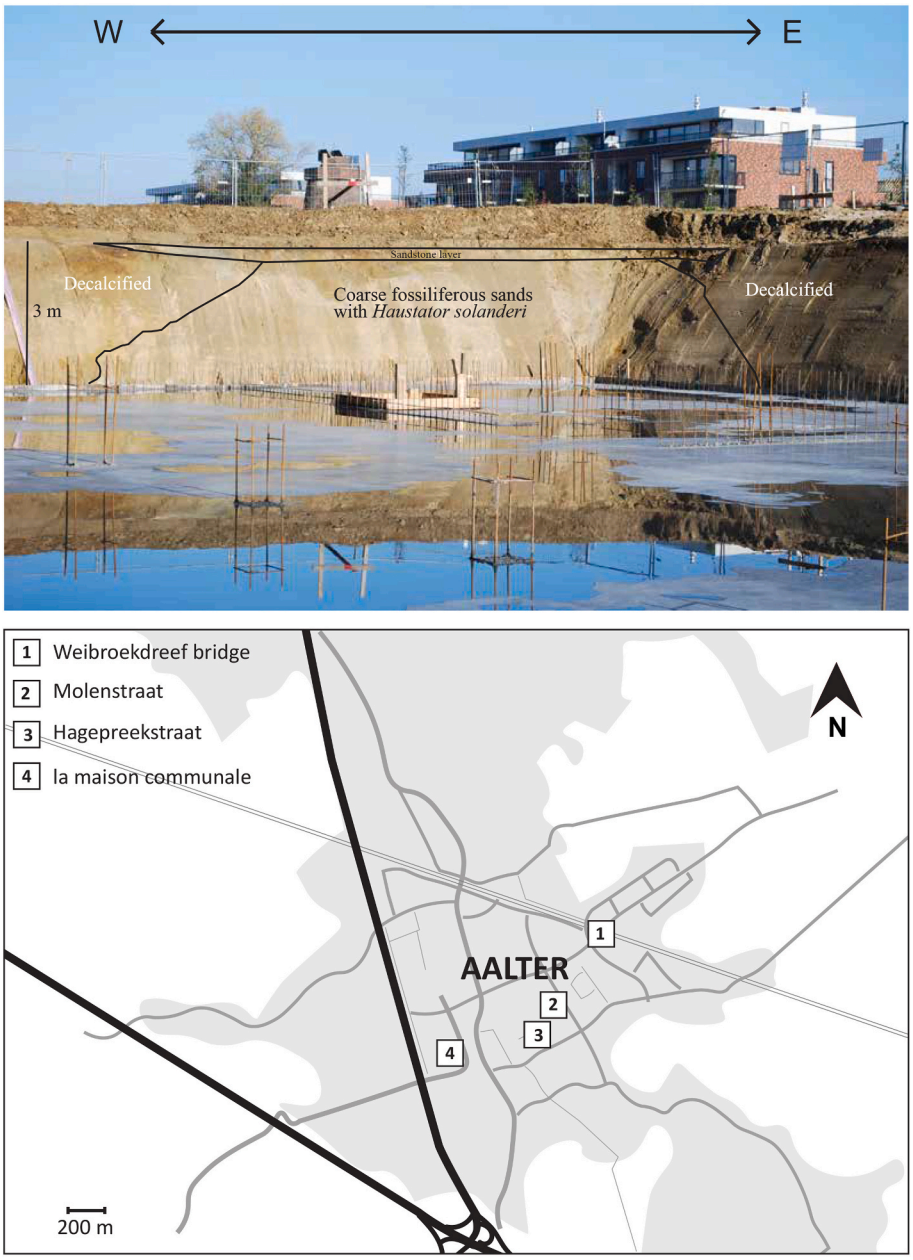

Appendix A1. Photograph of sampling locality V324 ("Aalter Hagepreekstraat"), taken November 1, 2010. Samples were taken from the 'fossiliferous sands with *Haustator solanderi*', a non-decalcified part of the Aalter Fm. protected from infiltration of meteoric water by a 0.25 m thick sandstone layer

Appendix B. Preservation assessment

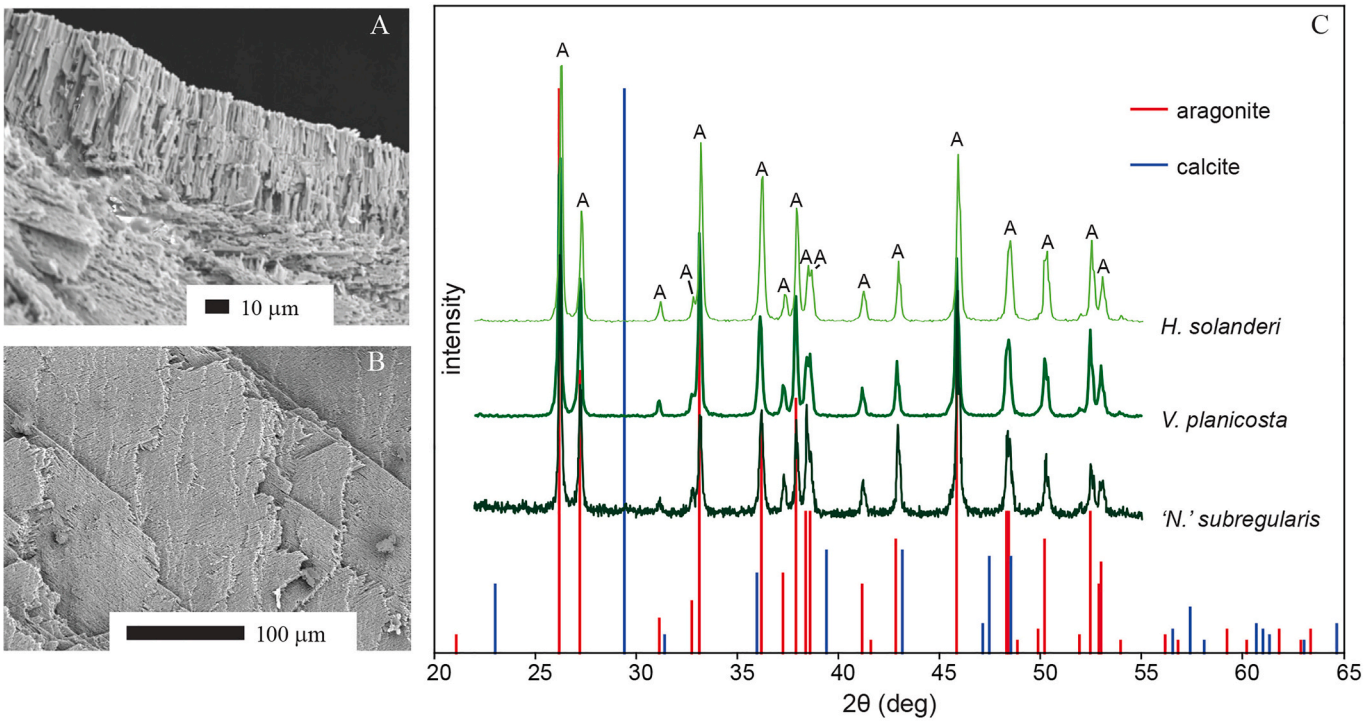

Appendix B1. SEM images of A) *H. solanderi* and B) *V. planicosta lerichei*, both from the Aalter Sand Fm. at Aalter, Belgium, and C) X-ray diffractograms of *H. solanderi*, *V. planicosta lerichei*, and *'N.' subregularis* from Aalter, showing the shells are composed of aragonite. Red vertical lines indicate diffraction angles associated with aragonite, while blue lines indicate angles associated with calcite diffraction. Image A) shows elongated crystals perpendicular to the shell surface. Image B) shows a plated ultrastructure. Structures are similar to those in modern mollusks and indicate that the original aragonite ultrastructure has been preserved

Appendix C. Supplementary data

Supplementary data to this article can be found online at https://doi.org/10.1016/j.palaeo.2024.112627.

References

Allmon, W.D., 1988. Ecology of recent turritelline gastropods (Prosobranchia, Turritellidae): current knowledge and paleontological implications. Palaios 3, 259–284. https://doi.org/10.2307/3514657.

Allmon, W.D., 2011. Natural history of turritelline gastropods (Cerithiodea: Turritellidae): a status report. Malacologia 54, 159–202. https://doi.org/10.4002/040.054.0107.

Allmon, W.D., Jones, D.S., Vaughan, N., 1992. Observations on the biology of *Turritella gonostoma* Valenciennes (Prosobranchia: Turritellidae) from the Gulf of California. Veliger 35, 52–63.

Anderson, B.M., Allmon, W.D., 2020. High calcification rates and inferred metabolic trade-offs in the largest turritellid gastropod, *Turritella abrupta* (Neogene). Palaeogeogr. Palaeoclimatol. Palaeoecol. 544, 109623. https://doi.org/10.1016/j.palaeo.2020.109623.

Andreasson, F.P., Schmitz, B., 1996. Winter and summer temperatures of the early middle Eocene of France from *Turritella* $\delta^{18}O$ profiles. Geology 24, 1067–1070. https://doi.org/10.1130/0091-7613(1996)024<1067:WASTOT>2.3.CO;2.

Andreasson, F.P., Schmitz, B., 1998. Tropical Atlantic seasonal dynamics in the early middle Eocene from stable oxygen and carbon isotope profiles of mollusk shells. Paleoceanography 13, 183–192. https://doi.org/10.1029/98PA00120.

Andreasson, F.P., Schmitz, B., 2000. Temperature seasonality in the early middle Eocene North Atlantic region: evidence from stable isotope profiles of marine gastropod shells. Geol. Soc. Am. Bull. 112, 628–640. https://doi.org/10.1130/0016-7606(2000)112<628:TSITEM>2.0.CO;2.

Austin, W.E.N., Cage, A.G., Scourse, J.D., 2006. Mid-latitude shelf seas: a NW European perspective on the seasonal dynamics of temperature, salinity and oxygen isotopes. The Holocene 16, 937–947. https://doi.org/10.1177/0959683606hl985rp.

Burke, K.D., Williams, J.W., Chandler, M.A., Haywood, A.M., Lunt, D.J., Otto-Bliesner, B. L., 2018. Pliocene and Eocene provide best analogs for near-future climates. Proc. Natl. Acad. Sci. 115, 13288–13293. https://doi.org/10.1073/pnas.1809600115.

Calvin, K., Dasgupta, D., Krinner, G., Mukherji, A., Thorne, P.W., Trisos, C., Romero, J., Aldunce, P., Barrett, K., Blanco, G., Cheung, W.W.L., Connors, S., Denton, F., Diongue-Niang, A., Dodman, D., Garschagen, M., Geden, O., Hayward, B., Jones, C., Jotzo, F., Krug, T., Lasco, R., Lee, Y.-Y., Masson-Delmotte, V., Meinshausen, M., Mintenbeck, K., Mokssit, A., Otto, F.E.L., Pathak, M., Pirani, A., Poloczanska, E., Pörtner, H.-O., Revi, A., Roberts, D.C., Roy, J., Ruane, A.C., Skea, J., Shukla, P.R., Slade, R., Slangen, A., Sokona, Y., Sörensson, A.A., Tignor, M., van Vuuren, D., Wei, Y.-M., Winkler, H., Zhai, P., Zommers, Z., Hourcade, J.-C., Johnson, F.X., Pachauri, S., Simpson, N.P., Singh, C., Thomas, A., Totin, E., Arias, P., Bustamante, M., Elgizouli, I., Flato, G., Howden, M., Méndez-Vallejo, C., Pereira, J. J., Pichs-Madruga, R., Rose, S.K., Saheb, Y., Sánchez Rodríguez, R., Ürge-Vorsatz, D., Xiao, C., Yassaa, N., Alegría, A., Armour, K., Bednar-Friedl, B., Blok, K., Cissé, G., Dentener, F., Eriksen, S., Fischer, E., Garner, G., Guivarch, C., Haasnoot, M., Hansen, G., Hauser, M., Hawkins, E., Hermans, T., Kopp, R., Leprince-Ringuet, N., Lewis, J., Ley, D., Ludden, C., Niamir, L., Nicholls, Z., Some, S., Szopa, S., Trewin, B., van der Wijst, K.-I., Winter, G., Witting, M., Birt, A., Ha, M., et al., 2023. In: Core writing Team, Lee, H., Romero, J. (Eds.), IPCC, 2023: Climate Change 2023: Synthesis Report. Contribution of Working groups I, II and III to the Sixth Assessment Report of the Intergovernmental Panel on climate Change. Intergovernmental Panel on Climate Change, Geneva, Switzerland. https://doi.org/10.59327/IPCC/AR6-9789291691647.

Cangzi, L., Walker, H.J., 1989. Sedimentary characteristics of cheniers and the formation of the chenier plains of East China. J. Coast. Res. 5, 353–368.

Clark, A.J., Vellekoop, J., Speijer, R.P., 2022. Hydrological differences between the Lutetian Paris and Hampshire basins revealed by stable isotopes of conid gastropods. Earth Sci. Bull. 193, 3. https://doi.org/10.1051/bsgf/2022002.

De Man, E., Ivany, L.C., Vandenberghe, N., 2004. Stable oxygen isotope record of the Eocene-Oligocene transition in the southern North Sea Basin: positioning the Oi-1 event. Neth. J. Geosci. 83, 193–197. https://doi.org/10.1017/S0016774600020266.

De Winter, N.J., 2022. ShellChron 0.4.0: a new tool for constructing chronologies in accretionary carbonate archives from stable oxygen isotope profiles. Geosci. Model Dev. 15, 1247–1267. https://doi.org/10.5194/gmd-15-1247-2022.

De Winter, N.J., Vellekoop, J., Vorsselmans, R., Golreihan, A., Soete, J., Petersen, S.V., Meyer, K.W., Casadio, S., Speijer, R.P., Claeys, P., 2018. An assessment of latest cretaceous *Pycnodonte vesicularis* (Lamarck, 1806) shells as records for palaeoseasonality: a multi-proxy investigation. Clim. Past 14, 725–749. https://doi.org/10.5194/cp-14-725-2018.

De Winter, N.J., Vellekoop, J., Clark, A.J., Stassen, P., Speijer, R.P., Claeys, P., 2020. The giant marine gastropod *Campanile giganteum* (Lamarck, 1804) as a high-resolution archive of seasonality in the Eocene greenhouse world. Geochem. Geophys. Geosyst. 21. https://doi.org/10.1029/2019GC008794.

De Winter, N.J., Witbaard, R., Kocken, I.J., Müller, I.A., Guo, J., Goudsmit, B., Ziegler, M., 2022. Temperature dependence of clumped isotopes (Δ_{47}) in aragonite. Geophys. Res. Lett. 49. https://doi.org/10.1029/2022GL099479.

De Winter, N.J., Tindall, J., Johnson, A.L.A., Goudsmit-Harzevoort, B., Wichern, N., Kaskes, P., Claeys, P., Huygen, F., van Leeuwen, S., Metcalfe, B., Bakker, P., Goolaerts, S., Wesselingh, F., Ziegler, M., 2024. Amplified seasonality in western Europe in a warmer world. Sci. Adv. 10, eadl6717. https://doi.org/10.1126/sciadv.adl6717.

Deshayes, G.P., 1858. P.: Description des animaux sans vertèbres découverts dans le bassin de Paris. Mollusques Acéphalés I 393–704, 3 In 4, Paris.

Dominici, S., Kowalke, T., 2014. Early Eocene Cerithioidean gastropods of mangrove-fringed coasts (South-central Pyrenees, Spain). Boll. Della Soc. Paleontol. Ital. 53, 137–162.

Dong, Y., Liao, M., Han, G., Somero, G.N., 2022. An integrated, multi-level analysis of thermal effects on intertidal molluscs for understanding species distribution patterns. Biol. Rev. 97, 554–581. https://doi.org/10.1111/brv.12811.

Eiler, J.M., 2007. "Clumped-isotope" geochemistry—the study of naturally-occurring, multiply-substituted isotopologues. Earth Planet. Sci. Lett. 262, 309–327. https://doi.org/10.1016/j.epsl.2007.08.020.

Evans, D., Sagoo, N., Renema, W., Cotton, L.J., Müller, W., Todd, J.A., Saraswati, P.K., Stassen, P., Ziegler, M., Pearson, P.N., Valdes, P.J., Affek, H.P., 2018. Eocene greenhouse climate revealed by coupled clumped isotope-Mg/ca thermometry. Proc. Natl. Acad. Sci. 115, 1174–1179. https://doi.org/10.1073/pnas.1714744115.

FishBase, 2023. https://www.fishbase.org last access: 7 August 2023.

Gély, J.-P., 2008. La stratigraphie et la paléogéographie du Lutétien en France. In: Merle, D. (Ed.), Stratotype Lutétien. MNHN/BRGM, Paris/Orléans, pp. 182–227.

Gibbard, P.L., Lewin, J., 2016. Filling the North Sea Basin: cenozoic sediment sources and river styles. Geol. Belg. 19, 201–217. https://doi.org/10.20341/gb.2015.017.

Gilbert, M., van de Poel, L., 1970. Les Bivalvia fossiles du Cénozoïque etranger des collections de 1'Institut royal des Sciences naturelles de Belgique, 6. Oligodontina, 2: Solenacea, Mactracea, Cardiacea - Astartedontina et Septibranchida. Memoires de l'Institut royal des Sciences naturelles de Belgique, 84, pp. 1–185.

Gillikin, D.P., Lorrain, A., Bouillon, S., Willenz, P., Dehairs, F., 2006. Stable carbon isotopic composition of *Mytilus edulis* shells: relation to metabolism, salinity, $\delta^{13}C_{DIC}$ and phytoplankton. Org. Geochem. 37, 1371–1382. https://doi.org/10.1016/j.orggeochem.2006.03.008.

Glibert, M., 1985. Les bivalves et gasteropodes du Bruxellien inferieur de la Belgique (Eocene moyen). Ann. Soc. R. Zool. Belg. 115, 261–367.

Goodwin, D.H., Flessa, K.W., Schone, B.R., Dettman, D.L., 2001. Cross-calibration of daily growth increments, stable isotope variation, and temperature in the Gulf of California bivalve mollusk *Chione cortezi*: implications for paleoenvironmental analysis. Palaios 16, 387–398. https://doi.org/10.1669/0883-1351(2001)016<0387:CCODGI>2.0.CO;2.

Goodwin, D.H., Schone, B.R., Dettman, D.L., 2003. Resolution and fidelity of oxygen isotopes as paleotemperature proxies in bivalve mollusk shells: models and observations. Palaios 18, 110–125. https://doi.org/10.1669/0883-1351(2003)18<110:RAFOOI>2.0.CO;2.

Grossman, E.L., Ku, T.-L., 1986. Oxygen and carbon isotope fractionation in biogenic aragonite: temperature effects. Chem. Geol. Isot. Geosci. Sect. 59, 59–74. https://doi.org/10.1016/0168-9622(86)90057-6.

Huyghe, D., Merle, D., Lartaud, F., Cheype, E., Emmanuel, L., 2012. Middle Lutetian climate in the Paris Basin: implications for a marine hotspot of paleobiodiversity. Facies 58, 587–604. https://doi.org/10.1007/s10347-012-0307-3.

Immenhauser, A., Schoene, B.R., Hoffmann, R., Niedermayr, A., 2016. Mollusc and brachiopod skeletal hard parts: Intricate archives of their marine environment. Sedimentology 63 (1), 1–59.

Ivany, L.C., 2012. Reconstructing paleoseasonality from accretionary skeletal carbonates—challenges and opportunities. Paleontol. Soc. Pap. 18, 133–166. https://doi.org/10.1017/S108933260000259X.

Ivany, L.C., Judd, E.J., 2022. Deciphering temperature seasonality in Earth's ancient oceans. Annu. Rev. Earth Planet. Sci. 50, 123–152. https://doi.org/10.1146/annurev-earth-032320-095156.

Ivany, L.C., Patterson, W.P., Lohmann, K.C., 2000. Cooler winters as a possible cause of mass extinctions at the Eocene/Oligocene boundary. Nature 407, 887–890. https://doi.org/10.1038/35038044.

Ivany, L.C., Lohmann, K.C., Hasiuk, F., Blake, D.B., Glass, A., Aronson, R.B., Moody, R. M., 2008. GSA Bulletin 120 (5–6), 659–678. https://doi.org/10.1130/B26269.1.

Ivany, L.C., Lohmann, K.C., Patterson, W., 2003. P.: Paleogene temperature history of the US Gulf Coastal Plain inferred from fossil otoliths. In: From Greenhouse to Icehouse: The Marine Eocene-Oligocene Transition. Columbia University Press, New York, pp. 232–251.

Ivany, L.C., Wilkinson, B.H., Lohmann, K.C., Johnson, E.R., McElroy, B.J., Cohen, G., 2004. J.: Intra-annual isotopic variation in *Venericardia* bivalves: Implications for early Eocene temperature, seasonality, and salinity on the U.S. Gulf Coast. J. Sediment. Res. 74, 7–19. https://doi.org/10.1306/052803740007.

Ivany, L.C., Pietsch, C., Handley, J.C., Lockwood, R., Allmon, W.D., Sessa, J.A., 2018. Little lasting impact of the Paleocene-Eocene thermal Maximum on shallow marine molluscan faunas. Sci. Adv. 4, eaat5528. https://doi.org/10.1126/sciadv.aat5528.

Jacobs, P., 2015. Hoofdstuk 3.4 Het midden-Eoceen en laat-Eoceen. In: Borremans, M. (Ed.), Geologie van Vlaanderen. Academia Press, Gent, p. 492.

Jacobs, P., De Batist, M., 1996. Sequence stratigraphy and architecture on a ramp-type continental shelf: the Belgian Palaeogene. In: De Batist, M., Jacobs, P. (Eds.), Geology of Siliciclastic Shelf Seas, 117. Geological Society, London, pp. 23–48. https://doi.org/10.1144/GSL.SP.1996.117.01.03. Special Publications.

Jacobs, P., Geets, S., 1977. Nieuwe ontwikkelingen in de kennis van het Boven-Paniseliaan. Natuurwetenschappelijk Tijdschr. 59, 57–93.

Jacobs, P., Sevens, E., 1993. Eocene siliciclastic continental shelf sedimentation in the Southern Bight North Sea, Belgium. In: Progress in Belgian Oceanographic Research, Brussels, p. 287. Jan. 21–22, 1993, Brussels.

Jacobs, P., Sevens, E., De Batist, M., Henriet, J.P., 1991. Grain-size, facies and sequence analysis of West Belgian Eocene continental shelf deposits. Zentralblatt Geol. Paläontol. Teil I (8), 931–955.

Jones, D.S., 1998. Isotopic determination of growth and longevity in fossil and modern invertebrates. Paleontol. Soc. Pap. 4, 37–67. https://doi.org/10.1017/S1089332600000395.

Jones, D.S., Allmon, W.D., 1995. Records of upwelling, seasonality and growth in stable-isotope profiles of Pliocene mollusk shells from Florida. Lethaia 28, 61–74. https://doi.org/10.1111/j.1502-3931.1995.tb01593.x.

Judd, E.J., Wilkinson, B.H., Ivany, L.C., 2018. The life and time of clams: Derivation of intra-annual growth rates from high-resolution oxygen isotope profiles. Palaeogeogr. Palaeoclimatol. Palaeoecol. 490, 70–83. https://doi.org/10.1016/j.palaeo.2017.09.034.

Kaasschieter, J.P.H., 1961. Foraminifera of the Eocene of Belgium. Mém. Inst. Roy. Sci. Nat. Belg. 147, 271.

Kanazawa, R.H., 1961. *Paraconger*, a new genus with three new species of eels (family Congridae). Proc. U. S. Natl. Mus. 113, 1–14. https://doi.org/10.5479/si.00963801.113-3450.1.

Keating-Bitonti, C.R., Ivany, L.C., Affek, H.P., Douglas, P., Samson, S.D., 2011. Warm, not super-hot, temperatures in the early Eocene subtropics. Geology 39, 771–774. https://doi.org/10.1130/G32054.1.

King, C., 2006. Paleogene and Neogene: uplift and a cooling climate. In: Brenchley, P.J., Rawson, P.F. (Eds.), The Geology of England and Wales. The Geological Society of London, pp. 395–427. https://doi.org/10.1144/GOEWP.16.

King, C., 2016. In: Gale, A.S., Barry, T.L. (Eds.), A Revised Correlation of Tertiary Rocks in the British Isles and Adjacent Areas of NW Europe, First. The Geological Society of London, p. 719. https://doi.org/10.1144/SR27.

Kniest, J.F., Davies, A.J., Brugger, J., Fiebig, J., Bernecker, M., Todd, J.A., Hickler, T., Voigt, S., Woodland, A., Raddatz, J., 2024. Dual clumped isotopes from Mid-Eocene bivalve shell reveal a hot and summer wet climate of the Paris Basin. Nat. Commun. Earth Environ. 5, 330. https://doi.org/10.1038/s43247-024-01491-8.

Knox, R.W.O., Bosch, J.H.A., Rasmussen, E.S., Heilmann-Clausen, E.S., Hiss, M., de Lugt, I.R., Kasiński, J., King, C., Köthe, A., Słodkowska, B., Standke, G., Vandenberghe, N., 2010. Cenozoic. In: Doornenbal, J.C., Stevenson, A.G. (Eds.), Petroleum Geological Atlas of the Southern Permian Basin Area. EAGE Publications, Houten, pp. 211–223.

Kobashi, T., Grossman, E.L., Yancey, T.E., Dockery, D.T., 2001. Reevaluation of conflicting Eocene tropical temperature estimates: molluskan oxygen isotope evidence for warm low latitudes. Geology 29, 983. https://doi.org/10.1130/0091-7613(2001)029<0983:ROCETT>2.0.CO;2.

Kobashi, T., Grossman, E.L., Dockery, D.T., Ivany, L.C., 2004. Water mass stability reconstructions from greenhouse (Eocene) to icehouse (Oligocene) for the northern Gulf Coast continental shelf (USA). Paleoceanography 19, PA1022. https://doi.org/10.1029/2003PA000934.

Lartaud, F., Emmanuel, L., de Rafelis, M., Pouvreau, S., Renard, M., 2010. Influence of food supply on the $\delta^{13}C$ signature of mollusc shells: implications for palaeoenvironmental reconstructions. Geo-Mar. Lett. 30, 23–34. https://doi.org/10.1007/s00367-009-0148-4.

Latal, C., Piller, W.E., Harzhauser, M., 2006. Shifts in oxygen and carbon isotope signals in marine molluscs from the Central Paratethys (Europe) around the lower/Middle Miocene transition. Palaeogeogr. Palaeoclimatol. Palaeoecol. 231, 347–360. https://doi.org/10.1016/j.palaeo.2005.08.008.

Le Bot, S., Van Lancker, V., Deleu, S., De Batist, M., Henriet, J.P., 2003. Tertiary and Quaternary Geology of the Belgian continental shelf. PPS Science Policy Publication, Brussels, pp. 1–76.

Lin, C.-H., Nolf, D., Steurbaut, E., Girone, A., 2017. Fish otoliths from the Lutetian of the Aquitaine Basin (SW France), a breakthrough in the knowledge of the European Eocene ichthyofauna. J. Syst. Palaeontol. 15, 879–907. https://doi.org/10.1080/14772019.2016.1246112.

Martens, L., Stassen, P., Steurbaut, E., Speijer, R.P., 2022. Assessing *Nummulites* geochemistry as a proxy for early Eocene palaeotemperature evolution in the North Sea Basin. J. Geol. Soc. Lond. 179, 2021–2102. https://doi.org/10.1144/jgs2021-102.

Mayer-Eymar, C., 1877. Paläontologie der Pariserstufe von Einsiedeln und seinen Umgebungen. Beiträge Geologischen Karte Schweiz 14 (2b), 1–100.

McConnaughey, T.A., Gillikin, D.P., 2008. Carbon isotopes in mollusk shell carbonates. Geo-Mar. Lett. 28, 287–299. https://doi.org/10.1007/s00367-008-0116-4.

Meckler, A.N., Sexton, P.F., Piasecki, A.M., Leutert, T.J., Marquardt, J., Ziegler, M., Agterhuis, T., Lourens, L.J., Rae, J.W.B., Barnet, J., Tripati, A., Bernasconi, S.M., 2022. Cenozoic evolution of deep ocean temperature from clumped isotope thermometry. Science 377, 86–90. https://doi.org/10.1126/science.abk0604.

Murray, J.W., 1992. Palaeogene and neogene. In: Cope, J.C.W., Ingham, J.K., Rawson, P. F. (Eds.), Atlas of Palaeogeography and Lithofacies. Geological Society of London, London, pp. 141–147.

Nolf, D., 1972a. Stratigraphie des formations du Panisel et de Den Hoorn (Eocène belge). Bull. Soc. Belge Géol. 81, 75–94.

Nolf, D., 1972b. Sur la faune ichthyologique des Formations du Panisel et de Den Hoorn (Eocène belge). Bull. Soc. Belge Géol. Paléontol. Hydrol. 81, 111–138.

Nolf, D., 1985. Otolithi piscium. In: Schultze, H.P. (Ed.), Handbook of Paleoichthyology, vol. 10. Fischer, Stuttgart & New York, pp. 1–145.

Nolf, D., 1995. Studies on fossil otoliths - The state of the art. In: Secor, D.H., Dean, J.M., Campana, S.E. (Eds.), Recent Developments in Fish Otolith Research, vol. 13. University of South Carolina Press, pp. 513–544.

Nyst, H., Mourlon, M., 1871. Note sur le gîte fossilifère d'Aeltre (flandre orientale). Mém. Société R. Malacol. Belg. 6, 29–37.
Peterson, B.J., Fry, B., 1987. Stable isotopes in ecosystem studies. Annu. Rev. Ecol. Syst. 293–320.
Pilling, G.M., Millner, R.S., Easey, M.W., Maxwell, D.L., Tidd, A.N., 2007. Phenology and North Sea cod *Gadus morhua* L.: has climate change affected otolith annulus formation and growth? J. Fish Biol. 70, 584–599. https://doi.org/10.1111/j.1095-8649.2007.01331.x.
Priem, F., 1906. Sur les Otolithes des Poissons éocènes du Bassin parisien. Bull. Soc. Géol. Fr. 4 (6), 265–280.
Purton, L.M.A., Brasier, M.D., 1999. Giant protist *Nummulites* and its Eocene environment: Life span and habitat insights from $\delta^{18}O$ and $\delta^{13}C$ data from *Nummulites* and *Venericardia,* Hampshire basin, UK. Geology 27, 711. https://doi.org/10.1130/0091-7613(1999)027<0711:GPNAIE>2.3.CO;2.
Purton, L.M.A., Shields, G.A., Brasier, M.D., Grime, G.W., 1999. Metabolism controls Sr/ca ratios in fossil aragonitic mollusks. Geology 27, 1083–1086. https://doi.org/10.1130/0091-7613(1999)027<1083:MCSCRI>2.3.CO;2.
Roberts, C.D., LeGrande, A.N., Tripati, A.K., 2009. Climate sensitivity to Arctic seaway restriction during the early Paleogene. Earth Planet. Sci. Lett. 286, 576–585. https://doi.org/10.1016/j.epsl.2009.07.026.
Rohling, E.J., 2013. Oxygen isotope composition of seawater. In: Encyclopedia of Quaternary Science. Elsevier, pp. 915–922. https://doi.org/10.1016/B978-0-444-53643-3.00293-4.
Schubert, R.J., 1916. Obereocane Otolithen vom Barton Cliff bei Christchurch (Hampshire). Jb. Geai. Reichsanst. 65, 277–288.
Schwarcz, H.P., Gao, Y., Campana, S., Browne, D., Knyf, M., Brand, U., 1998. Stable carbon isotope variations in otoliths of Atlantic cod (*Gadus morhua*). Can. J. Fish. Aquat. Sci. 55, 1798–1806. https://doi.org/10.1139/f98-053.
Schwartzmann, C., Durrieu, G., Sow, M., Ciret, P., Lazareth, C.E., Massabuau, J.-C., 2011. In situ giant clam growth rate behavior in relation to temperature: a one-year coupled study of high-frequency noninvasive valvometry and sclerochronology. Limnol. Oceanogr. 56, 1940–1951. https://doi.org/10.4319/lo.2011.56.5.1940.
Sessa, J.A., Ivany, L.C., Schlossnagle, T.H., Samson, S.D., Schellenberg, S.A., 2012. The fidelity of oxygen and strontium isotope values from shallow shelf settings: Implications for temperature and age reconstructions. Palaeogeogr. Palaeoclimatol. Palaeoecol. 342–343, 27–39. https://doi.org/10.1016/j.palaeo.2012.04.021.
Smith, D.G., 1989. Family congridae. In: Böhlke, E.B. (Ed.), Fishes of the Western North Atlantic. Part 9, vol. 1. Sears Foundation for Marine Research, Yale University, New Haven, pp. 460–567.
Solomon, C.T., Weber, P.K., Cech Jr., J.J., Ingram, B.L., Conrad, M.E., Machavaram, M. V., Pogodina, A.R., Franklin, R.L., 2006. Experimental determination of the sources of otolith carbon and associated isotopic fractionation. Can. J. Fish. Aquat. Sci. 63, 79–89. https://doi.org/10.1139/f05-200.
Speijer, R.P., Pälike, H., Hollis, C.J., Hooker, J.J., Ogg, J.G., 2020. The paleogene period. In: Geologic Time Scale 2020. Elsevier, pp. 1087–1140. https://doi.org/10.1016/B978-0-12-824360-2.00028-0.
Steurbaut, E., 2006. Ypresian. Geol. Belg. 9, 73–93.
Steurbaut, E., 2011. New calcareous nannofossil taxa from the Ypresian (early Eocene) of the North Sea Basin and the Turan Platform in West Kazakhstan. Bull. Roy. Belg. Inst. Nat. Sci. Aardwetenschappen 81, 247–277.
Steurbaut, E., 2015. Het vroeg-Eoceen. In: Borremans, M. (Ed.), Geologie van Vlaanderen. Academia Press Gent, pp. 125–135.
Steurbaut, E., Nolf, D., 1989. The stratotype of the Aalter Sands (Eocene of NW Belgium): stratigraphy and calcareous nannoplankton. Meded. Werkgr. Tert. Kwart. Geol. 26, 11–28.
Steurbaut, E., Nolf, D., 1990. Ypresian teleost otoliths from Belgium and northwestern France. Bull. Soc. Belge Géol. 97, 321–347.
Steurbaut, E., Nolf, D., 2021. The Mont-des-Récollets section (N France): a key site for the Ypresian-Lutetian transition at mid-latitudes – reassessment of the boundary criterion for the base-Lutetian GSSP. Geodiversitas 43. https://doi.org/10.5252/geodiversitas2021v43a11.
Steurbaut, E., De Coninck, J., Van Simaeys, S., 2016. Micropalaeontological dating of the Prémontré mammal fauna (MP10, Prémontré Sands, EECO, early late Ypresian, Paris Basin). Geol. Belg. 19, 273–280. https://doi.org/10.20341/gb.2016.006.
Strauss, J., Oleinik, A., Swart, P., 2014. Stable isotope profiles from subtropical marine gastropods of the family Fasciolariidae: growth histories and relationships to local environmental conditions. Mar. Biol. 161, 1593–1602. https://doi.org/10.1007/s00227-014-2443-5.
Takai, N., Mishima, Y., Yorozu, A., Hoshika, A., 2002. Carbon sources for demersal fish in the western Seto Inland Sea, Japan, examined by $\delta^{13}C$ and $\delta^{15}N$ analyses. Limnol. Oceanogr. 47, 730–741. https://doi.org/10.4319/lo.2002.47.3.0730.
Teusch, K.P., Jones, D.S., Allmon, W.D., 2002. Morphological variation in turritellid gastropods from the Pleistocene to recent of Chile: association with upwelling intensity. Palaios 17, 366–377. https://doi.org/10.1669/0883-1351(2002)017<0366:MVITGF>2.0.CO;2.
Tierney, J.E., Poulsen, C.J., Montañez, I.P., Bhattacharya, T., Feng, R., Ford, H.L., Hönisch, B., Inglis, G.N., Petersen, S.V., Sagoo, N., Tabor, C.R., Thirumalai, K., Zhu, J., Burls, N.J., Foster, G.L., Goddéris, Y., Huber, B.T., Ivany, L.C., Kirtland Turner, S., Lunt, D.J., McElwain, J.C., Mills, B.J.W., Otto-Bliesner, B.L., Ridgwell, A., Zhang, Y.G., 2020. Past climates inform our future. Science 370, eaay3701. https://doi.org/10.1126/science.aay3701.
Tindall, J., Flecker, R., Valdes, P., Schmidt, D.N., Markwick, P., Harris, J., 2010. Modelling the oxygen isotope distribution of ancient seawater using a coupled ocean–atmosphere GCM: implications for reconstructing early Eocene climate. Earth Planet. Sci. Lett. 292, 265–273. https://doi.org/10.1016/j.epsl.2009.12.049.
Tohse, H., Mugiya, Y., 2008. Sources of otolith carbonate: experimental determination of carbon incorporation rates from water and metabolic CO2, and their diel variations. Aquat. Biol. 1, 259–268. https://doi.org/10.3354/ab00029.
Ullmann, C.V., Wiechert, U., Korte, C., 2010. Oxygen isotope fluctuations in a modern North Sea oyster (*Crassostrea gigas*) compared with annual variations in seawater temperature: Implications for palaeoclimate studies. Chem. Geol. 277, 160–166. https://doi.org/10.1016/j.chemgeo.2010.07.019.
Van Hinsbergen, D.J.J., de Groot, L.V., van Schaik, S.J., Spakman, W., Bijl, P.K., Sluijs, A., Langereis, C.G., Brinkhuis, H., 2015. A paleolatitude calculator for paleoclimate studies. PLoS ONE 10 (6). https://doi.org/10.1371/journal.pone.0126946.
Van Horebeek, N., Vellekoop, J., Clark, A.J., Speijer, R.P., 2021. Changing life mode of *Campanile giganteum* (Lamarck, 1804) with age: shifting habitat or food sources?. In: Geologica Belgica Conference Proceedings, 7th International Geologica Belgica Meeting 2021, Tervuren, Belgium, p. 376. https://doi.org/10.20341/gbcp.vol4.
Vandenberghe, N., Van Simaeys, S., Steurbaut, E., Jagt, J.W.M., Felder, P.J., 2004. Stratigraphic architecture of the Upper cretaceous and Cenozoic along the southern border of the North Sea Basin in Belgium. Neth. J. Geosci. 83, 155–171. https://doi.org/10.1017/S0016774600020229.
Vanhove, D., Stassen, P., Speijer, R.P., Steurbaut, E., 2011. Assessing paleotemperature and seasonality during the early Eocene Climatic Optimum (EECO) in the Belgian Basin by means of fish otolith stable O and C isotopes. Geol. Belg. 14, 143–158.
Vanhove, D., Stassen, P., Speijer, R.P., Claeys, P., Steurbaut, E., 2012. Intra- and intertaxon stable O and C isotope variability of fossil fish otoliths: an early Eocene test case. Austr. J. Earth Sci. 105, 200–207.
Versteegh, E.A.A., Vonhof, H.B., Troelstra, S.R., Kaandorp, R.J.G., Kroon, D., 2010. Seasonally resolved growth of freshwater bivalves determined by oxygen and carbon isotope shell chemistry. Geochem. Geophys. Geosyst. 11. https://doi.org/10.1029/2009GC002961.
Waite, R., Allmon, W.D., 2013. Observations on the biology and sclerochronology of *Turritella leucostoma* (Valenciennes, 1832; Cerithioidea: Turritellidae) from the Gulf of California. Am. Malacol. Bull. 31, 297–310. https://doi.org/10.4003/006.031.0209.
Wefer, G., Berger, W.H., 1991. Isotope paleontology: growth and composition of extant calcareous species. Mar. Geol. 100, 207–248. https://doi.org/10.1016/0025-3227(91)90234-U.
Westerhold, T., Röhl, U., Donner, B., Zachos, J.C., 2018. Global extent of early eocene hyperthermal events: a new pacific benthic foraminiferal isotope record from shatsky rise (ODP site 1209). Paleoceanogr. Paleoclimatol. 33, 626–642. https://doi.org/10.1029/2017PA003306.
Williams, D.F., Arthur, M.A., Jones, D.S., Williams, N.H., 1982. Seasonality and mean annual sea surface temperatures from isotopic and sclerochronological records. Nature 296, 432–434.
Wurster, C.M., Patterson, W.P., 2001. Late Holocene climate change for the eastern interior United States: evidence from high-resolution δ18O values of sagittal otoliths. Palaeogeogr. Palaeoclimatol. Palaeoecol. 170, 81–100. https://doi.org/10.1016/S0031-0182(01)00229-2.
Yonge, C.M., 1969. Functional morphology and evolution within the Carditacea (Bivalvia). Proc. Malacol. Soc. Lond. 38, 493–527. https://doi.org/10.1093/oxfordjournals.mollus.a065067.
Zachos, J.C., Stott, L.D., Lohmann, K.C., 1994. Evolution of early Cenozoic marine temperatures. Paleoceanography 9, 353–387. https://doi.org/10.1029/93PA03266.
Zachos, J.C., Dickens, G.R., Zeebe, R.E., 2008. An early Cenozoic perspective on greenhouse warming and carbon-cycle dynamics. Nature 451, 279–283. https://doi.org/10.1038/nature06588.
Zhu, J., Poulsen, C.J., Otto-Bliesner, B.L., Liu, Z., Brady, E.C., Noone, D.C., 2020. Simulation of early Eocene water isotopes using an Earth system model and its implication for past climate reconstruction. Earth Planet. Sci. Lett. 537, 116164. https://doi.org/10.1016/j.epsl.2020.116164.